The cellular localisation of avian influenza virus PB1-F2 protein alters the magnitude of IFN2 promoter and NFκB-dependent promoter antagonism in chicken cells.

Running title: PB1-F2 localisation alters innate signaling antagonism in chickens.

Joe James[a,b,c], Nikki Smith[d], Craig Ross[e], Munir Iqbal[a], Steve Goodbourn[e], Paul Digard[d], Wendy S. Barclay[b] and Holly Shelton[a#]

[a]The Pirbright Institute, Pirbright, Woking, UK [b]Imperial College London, UK, [c] Current address; APHA, Weybridge, UK, [d]The Roslin Institute, Edinburgh, UK, [e] St George's, University of London, UK.

#Corresponding author: Holly Shelton, Holly.Shelton@Pirbright.ac.uk. The Pirbright Institute, Pirbright, Surrey, UK[a]. T: +44 (0) 1483 231492

Keywords: Influenza virus, PB1-F2, IKKβ, MAVS, chicken

Abstract word count: 235

Main body word count: 7350

Abstract

The accessory protein, PB1-F2, of influenza A virus (IAV) functions in a chicken host to prolong infectious virus shedding and thus the transmission window. Here we show that this delay in virus clearance by PB1-F2 in chickens is accompanied by reduced transcript levels of type 1 interferon (IFN) induced genes and NFκB activated pro-inflammation cytokines. *In vitro* two avian influenza isolate derived PB1-F2 proteins, H9N2 UDL01 and H5N1 5092, exhibited the same antagonism of the IFN and pro-inflammation induction pathways seen *in vivo* but to different extents. The two PB1-F2 proteins had different cellular localisation in chicken cells, H5N1 5092 being predominantly mitochondrial associated and H9N2 UDL being cytoplasmic but not mitochondrial localized. We hypothesized that PB1-F2 localisation might influence the functionality of the protein during infection and that protein sequence could alter cellular localisation. We demonstrate that the sequence of the C-terminus of PB1-F2 determined cytoplasmic localisation, in chicken cells and this was linked with protein instability. Mitochondrial localization of PB1-F2 resulted in reduced antagonism of an NFκB-dependent promoter. In parallel mitochondrial localisation of PB1-F2 increased the potency of chicken IFN 2 induction antagonism. We suggest mitochondrial localisation of PB1-F2 restricts interaction with cytoplasmic located IKKβ reducing NFκB responsive promoter antagonism but enhances antagonism of the IFN2 promoter through interaction with the mitochondrial adaptor MAVS. Our study highlights the differential mechanisms by which IAV PB1-F2 protein can dampen the avian host innate signaling response.

Introduction

Influenza A viruses (IAV) are respiratory pathogens of multiple species including poultry and humans. High prevalence levels of IAV infection in poultry in the Middle East and South East Asia, where it is considered endemic in some countries, causes a significant economic burden to the poultry industry [1, 2]. It is estimated that the H7N9 subtype of avian IAV caused upwards of $6.5 billion in losses to the Chinese economy in 2013 alone [3]. Food security, animal welfare and of course the potential spillover into the human population and the resulting possibility of pandemics, are all important reasons for further study of IAV interactions within avian hosts, with the aim of enabling the design and implementation of better control strategies for IAV in poultry.

IAVs have a core repertoire of 10 viral proteins that all subtypes express, allowing successful replication of the virus in infected cells. There is also an ever increasing number of 'accessory' proteins which are not required for replication in a cell, but which contribute and modulate IAV infection *in vivo* [4]. In 2001, PB1-F2 was the first accessory protein identified in IAV [5]. PB1-F2 is a small protein ranging in size from 87 -101 amino acids (aa) and expressed from genome segment 2 of IAV in a +1 reading frame relative to that of the PB1 protein, the viral RNA-dependent-RNA-polymerase [5]. The presence of PB1-F2 in the IAV genome is highly conserved, 93%, as a full length protein in IAV isolates recovered from avian species which contrasts with a full length conservation of only 43% in human or 48% in swine isolated IAV sequences [6, 7].

Many functions have been attributed to PB1-F2 since its identification; it has variously been shown to: induce apoptosis, antagonize innate immune responses, promote

secondary bacterial infection and modulate viral polymerase activity, but many of these functions have been shown to be cell type and IAV strain dependent [8, 9]. It has also been shown to be rapidly turned over in cells due to degradation by the proteosome [10].

Previously we and others have shown that the absence of a full length PB1-F2 protein in an avian IAV has the effect of increasing pathogenicity, in chickens, in both highly pathogenic and low pathogenic IAV infection models [6, 11]. It has been documented in mammalian models that IAV infections with large innate responses, characterized by extraordinary levels of inflammatory cytokines and chemokines, correlate with enhanced pathogenicity [12, 13]. Therefore the absence of PB1-F2 resulting in enhanced innate immune responses is a likely mechanism for this increase in pathogenicity in chickens. It has been previously demonstrated in mammalian cells infected with IAV that PB1-F2 can antagonize anti-viral innate responses, for example Yoshizumi *et al* (2014) and others report that human interferon beta (IFNβ) promoter activation is suppressed by the presence of PB1-F2 [14-17]. Additionally, *in vivo,* in mice, type 1 interferon (IFN) induced transcripts in the lung were reduced when PB1-F2 was present [18]. In chickens in the context of a highly pathogenic H5N1 IAV it was found that similar to mice, infection with a virus that contained a full-length PB1-F2 protein resulted in reduced levels of a range of anti-viral innate gene transcripts [11]. A direct interaction between PB1-F2 of the vaccine strain A/PR/8/34 (PR8) and human mitochondrial antiviral-signaling protein (MAVS) has been demonstrated by co-immunoprecipitation and it is thought that PB1-F2 exerts its antagonist function of mammalian IFNα/β through modulation of this critical adapter protein in the IFN induction pathway [19, 20]. Reis *et al* (2013) showed that PB1-F2 from a range of avian IAVs and PR8 were able to interact with human IKKβ, resulting

in inhibition of human NFκB activation. The antagonistic functionality of PB1-F2 for the interferon induced and pro-inflammation pathways in avian cell lines and hosts is less clear however with only one study providing data where the effect of PB1-F2 on transcript levels of interferon stimulated genes in the lungs of chickens infected with a highly pathogenic H5N1 strain was analysed [11]. Leymarie *et al* (2014), showed that transcripts of the interferon signaling pathway were down-regulated when comparing data sets from infections by a PB1-F2 containing virus and the isogenic knock-out of PB1-F2. Differences exist between the signaling induction pathways for innate response cytokines and chemokines in chickens and mammals, for example chickens lack the pattern recognition receptor RIG-I important for initiating the type 1 IFN induction pathway in mammals [21]. Sequence comparison between human MAVS and chicken MAVS shows only a 39% conservation at the amino acid level whereas there is a stronger degree of conservation between human IKKβ and that in the chicken genome (83% conservation at amino acid level). There has been no analysis of the mechanism of immune response suppression in the chicken host by PB1-F2. It is likely that host immune response suppression results in the observation our group previously reported, that the presence of a PB1-F2 protein, in a low pathogenic H9N2 IAV, can prolong the virus shedding duration in chickens, resulting in an increased transmission window and environmental contamination [6].

In mammalian cells PB1-F2 proteins display one of two sub-cellular localisations; predominantly mitochondrial associated as is the case for the PB1-F2 protein from the laboratory adapted H1N1 A/PR8/8/34 (PR8) or diffuse in the cytoplasm with a small proportion of mitochondrial localisation as is the case for H5N1 A/HK/156/1997 [5, 22-25]. However, no study of cellular localisation in avian cell types has been undertaken. It has

been noted in several reports that the C-terminus sequence of the PB1-F2 protein determines cellular localisation in mammalian cells, although the residues that confer mitochondrial targeting appear to vary between PB1-F2 proteins [22]. The ability of PB1-F2 to antagonize mammalian IFNα/ β promoters has been linked to the C-terminus of PB1-F2 [19, 20].

PB1-F2 protein of IAV is variable in sequence which has been shown to impact cellular localisation and function in mammalian cells. There is a paucity of published information about PB1-F2 in the context of IAV infection of avian cells and IAV isolates that infect avian species are more likely to have a full length PB1-F2 protein encoded in their genome. Therefore there is a particular gap in the knowledge of the specific *in vitro* functions of PB1-F2 in avian cells and how these might be correlated with the PB1-F2 effects on IAV pathogenicity and viral shedding in chickens.

Here we analysed the cellular localisation and ability of avian IAV PB1-F2 proteins to antagonize type 1 IFN, (IFN-1 and IFN-2) and pro-inflammation induction pathways in chicken cells. We demonstrate that the C-terminal sequence of PB1-F2 can alter the cellular localisation and that mitochondrial association of PB1-F2 affects antagonistic function and stability of PB1-F2 in chicken cells. We confirmed interactions with chicken orthologues of MAVs and IKKβ suggesting that PB1-F2 acts to suppress innate responses in chickens and this is the mechanism of suppressed pathogenicity and prolonged viral shedding of IAV strains that carry full length PB1-F2 proteins.

Results

PB1-F2 protein from different strains of avian influenza virus have distinct cellular localisations in chicken cells.

We analysed the association with mitochondria of PB1-F2, from a wide panel of different avian influenza virus subtypes (Table 1), in a chicken fibroblast cell line (Fig. 1). DF1 cells were transfected with plasmids encoding PB1-F2 proteins with an N-terminal V5 tag and immune stained for the V5 tag along with Mitotracker dye to highlight the mitochondria before imaging by confocal microscopy. Co-localisation between mitochondria and PB1-F2 was quantified by drawing transects through the mitochondria and determining the correlation of pixel intensity for PB1-F2 and mitochondrial staining using a Pearson's coefficient. Both visually and by quantification the PB1-F2 proteins could be categorised in two groups; those with strong mitochondrial co-localisation, having Pearson's coefficients of > 0.7, (H5N1 50-92, H3N8a, and H10N7), and those that showed a diffuse cytoplasmic localisation with a weak mitochondria association, having Pearson's coefficients of < 0.7, (H9N2 UDL01, H8N4, H11N9, H3N8b and H6N2).

Localisation of PB1-F2 in the cytoplasm is determined by amino acids in the C-terminus of the protein.

The PB1-F2 proteins of the viruses H9N2 UDL01 and H5N1 50-92 are examples which fell into the two different localisation patterns. H9N2 UDL01, $R^2 = 0.243$ (± 0.032 Standard Error of the Mean [SEM]) is predominantly cytoplasmic whereas H5N1 50-92, R2 = 0.749 (± 0.024 SEM) is predominantly mitochondria associated (Fig. 1 and Fig. 2(b)). A comparison of the primary amino acid sequences of H9N2 UDL01 and H5N1 50-92 PB1-

F2 proteins revealed that there were 11 amino acid differences between them, four in the N-terminal region (aa 1-35) and seven in the C-terminus (aa 41-90) (Fig. 2(a)). Previous reports have demonstrated that the association of PB1-F2 with mitochondria in mammalian cells is determined by the PB1-F2 C-terminus [17, 22, 23]. Therefore we generated chimeric PB1-F2 proteins whereby a swap of the C-terminus (aa 41-90) were made. We generated UDL01:5092 PB1-F2 which contained the N-terminus of H9N2 UDL01 and C-terminus of H5N1 50-92 and the reciprocal swap 5092:UDL01 PB1-F2 (Fig. 2(a)). Transects drawn through mitochondria on confocal microscopy images confirmed that V5-PB1-F2 localisation to the cytoplasm was determined by the C-terminus of the UDL01 PB1-F2 protein (Fig. 2(b)). However the H5N1 5092 C-terminus (UDL01:5092) did not enable localisation at the mitochondria to the same extent as the H5N1 5092 WT PB1-F2. The UDL01:5092 PB1-F2 protein was however more efficiently targeted to the mitochondria, with a mean R^2 correlation value of 0.648 (± 0.026 SEM) than compared to 5092:UDL01 which was predominantly cytoplasmic, the mean R^2 correlation value with mitochondria being 0.273 (± 0.045 SEM), (Fig. 2(b)). Previous publications have demonstrated that putative mitochondrial targeting sequences lie between amino acid residues 46 and 75. There were four residues that were different between our two prototypic strains in this aa 46-75 region so we generated expression constructs which swapped all four mutations in both the H9N2 UDL01 and H5N1 5092 PB1-F2 proteins to analyse in greater detail those residues that contribute to PB1-F2 localisation away from the mitochondria. Site directed mutagenesis at aa 60, 62, 66 and 68 (from R, H, N, I respectively) in H9N2 UDL01 to Q, L, S, T as is the sequence in H5N1 5092 generated the UDL01-4M PB1-F2 and the reverse mutations in H5N1 5092 generated the 5092-4M PB1-F2. Co-localisation of UDL01-4M and 5092-4M PB1-F2 proteins that were V5

tagged, with mitochondria via co-staining with Mitotraker Red in DF-1 cells demonstrated that the 5092-4M PB1-F2 was relocalised in a diffuse pattern to the cytoplasm ($R^2 = 0.399$) (Fig. 2(c)), similarly to UDL WT ($R^2 = 0.024$ (± 0.032 SEM)) and 5092:UDL01 ($R^2 = 0.273$ (± 0.045 SEM)). Conversely UDL01-4M PB1-F2 had no effect on mitochondrial localisation ($R^2 = 0.265$) (Fig. 2(c)) maintaining a similar diffuse cytoplasmic localisation to H9N2 UDL in contrast with the UDL01:5092 mutant ($R^2 = 0.647$ (± 0.045 SEM)). This suggests that mitochondrial targeting is more easily disrupted than the retargeting of PB1-F2 to the mitochondria which may require features in the full length protein. Sequence analysis of the region between aa 46-75 of the other avian influenza virus PB1-F2 proteins from Fig. 1, indicated that the 4 amino acids identified as important for the cytoplasmic localisation of the H5N1 5092-4M PB1-F2 are not in common in cytoplasmic targeted PB1-F2s. Indeed the PB1-F2 protein from H8N4 A/Mallard/Alberta/192/92 had a cytoplasmic localisation and shared identical residues at these 4 positions with H5N1 5092 which was mitochondrial targeted. None of the other PB1-F2 proteins shared the 60R, 62H, 66N, 68I motif seen in H9N2 UDL01, although the mitochondrial located PR8 PB1-F2 has 60R, 66N, 68I (Fig. 2(d)).

PB1-F2 supresses' interferon stimulated gene transcripts upon avian influenza virus infection in chicken cells.

To provide robust data on the functionality of PB1-F2 to antagonise the type I interferon signalling pathway in chickens we used several different methods. Firstly, we analysed and compared the transcript levels of ISGs in nasal tissue taken from chickens at two and five days post infection with isogenic H9N2 viruses that contain the coding capacity for either a full length PB1-F2 protein (H9N2 UDL01) or a truncation to the initial 11 aa of

PB1-F2 (H9N2 UDL01-KO), deemed to be non-functional and therefore a knock-out (Fig. 3(a)). These two viruses had previously been reported on in James *et al* (2016) and replicated in chicken tissues to similar levels on day two post infection but with the PB1-F2 knock out H9N2 infectious virus being cleared more quickly on day 5 than the H9N2 with a full length PB1-F2 protein (Supplementary Fig. 1) [6]. We observed significantly increased transcript levels for several ISGs and cytokines in the nasal tissue from birds infected by the H9N2 PB1-F2 knock-out virus on both day 2 (Mx, OAS, STAT-1, IL-6) and day 5 (Mx, IL-6, IL-1b) post infection (Fig. 3(a)).

We utilised primary chicken embryonic fibroblast (CEF) cells and chicken bone marrow derived monocyte (BMDM) cells to see whether the same upregulation of ISG and cytokine transcripts was observed *in vitro* by avian influenza viruses lacking a functional PB1-F2 protein compared to those possessing a full length PB1-F2 protein (Fig. 3(b) & (c)). In both cell types the H5N1 5092 virus pair (H5N1 5092 & H5N1 5092-KO) showed a significant increase in Mx and OAS transcript level when PB1-F2 was absent during infection and the trend was evident for the H9N2 UDL01 virus pair although not statistically significant. In the BMDM, transcript levels for IL-6 and IL-8 were significantly elevated when PB1-F2 was absent in the H9N2 UDL01-KO virus and again this trend was evident for the H5N1 5092 virus pair but it was not statistically significant. Both H9N2 UDL01 and H5N1 5092 virus pairs were equally able to infect both CEFs and BMDM at an MOI of 3 (Fig. 3(d) & (e)). Growth curves of the virus pairs in primary chicken kidney cells (Supplementary Fig. 4(a)) showed that for both pairs of viruses there was no difference in infectious virus release at early time points post infection, up to 24 hours. We did observe significantly more virus at 48 hours post infection in the growth curve for

the H5N1 5092 PB1-F2 KO virus compared to H5N1 5092 WT. In the chicken fibroblast DF-1 cell line reconstituted viral polymerase activity of both the H5N1 5092 and H9N2 UDL01 viruses was not affected by the ability of the PB1 segment to encode a full length PB1-F2 (Supplementary Fig. 4(b)). Our *in vitro* infections suggested that PB1-F2 of both H9N2 UDL01 and H5N1 5092 were able to suppress ISG and pro-inflammation cytokines transcripts but the potency of the antagonism varied. There was a trend in the *in vitro* tested substrates, CEFs and chicken BMDM, that the PB1-F2 of H5N1 5092 could more potently antagonise chicken IFN1 and IFN2 stimulated genes, Mx and OAS upon infection (a difference of 50-250 fold compared to H5N1 5092-KO) whereas the H9N2 UDL01 PB1-F2 displayed a more modest 20 fold difference compared with H9N2 UDL01-KO. In contrast the H9N2 UDL01 PB1-F2 more potently antagonised the pro-inflammation cytokines IL-6 and IL-8 compared to H5N1 5092 PB1-F2 upon infection (Fig. 3 (b-c)).

Co-localisation with the mitochondria and consequently MAVS enhances chicken IFN-2 promoter antagonism by PB1-F2.

We performed a colocalisation study in chicken DF-1 cells by overexpression of a V5-tagged chicken MAVS construct (ckMAVS-V5) and FLAG tagged version of the H9N2 UDL01 and H5N1 5092 PB1-F2 proteins (Fig. 4(a) and Supplementary Fig. 2). Similarly to the co-localisation with Mitotraker we performed immune staining against the FLAG and V5 tags and drew transect lines through the confocal images along the ckMAVS-V5 staining and the correlation of pixel intensity along these transects for each stain was then calculated using a Pearson's coefficient. We observed that mitochondrial targeted H5N1 5092 PB1-F2 protein had a strong colocalisation with ckMAVS (R^2 = 0.851 ±0.022 SEM) whereas the H9N2 UDL01 PB1-F2 protein only had a weak correlation (R^2 = 0.332 ±

0.042 SEM), a GFP-FLAG expression construct was used as a control and showed no co-localisation with ckMAVS-V5 (R^2 = -0.002 ± 0.020 SEM) (Fig. 4(a)). Co-immunoprecipitation using an anti-V5 antibody from DF-1 cells expressing ckMAVS-V5 and either FLAG tagged H5N1 5092 or H9N2 UDL01 PB1-F2 demonstrated that both PB1-F2 proteins could interact with ckMAVS but that the efficiency of binding differed, the H5N1 5092 PB1-F2 associating to a greater extent with ckMAVS than H9N2 UDL01 (Fig. 4(b)).

Having already detailed the cellular localisation difference of the PB1-F2 proteins, H9N2 UDL01 and H5N1 5092, we hypothesised that cellular localisation could influence the potency with which type 1 IFN was induced and consequently ISGs during infection. Therefore we used a well described IFN bioassay that makes use of type 1 IFN inhibition of a GFP vesicular stomatitis virus (VSV-GFP) to determine the ability of the PB1-F2 proteins to antagonise production of bioactive chicken IFN from DF-1 chicken cells [26]. We applied equal volumes of virus inactivated supernatant taken from chicken BMDM cells infected with H9N2 UDL01 and H5N1 5092 isogenic virus pairs that contained a full length PB1-F2 or PB1-F2 KO, at a high MOI to DF-1 cells, as a primer, prior to infection of the DF-1s by VSV-GFP. The level of GFP fluorescence measured in the cells was therefore inversely proportional to the relative levels of IFNs secreted during the initial influenza infection. We found that in both virus pairs the parental viruses that contained a full length PB1-F2 protein induced less type 1 IFN following infection than the viruses that were knocked out for PB1-F2 (Fig. 4(c)). This suggested that the level of IFN induction was more greatly suppressed by the PB1-F2 from H5N1 5092 which is located predominantly at the mitochondria, colocalised with ckMAVS than the PB1-F2 from H9N2

UDL01 which has a more modest colocalisation with MAVS and a predominantly cytoplasmic cellular localisation.

To increase the clarity of the relationship between subcellular localisation of PB1-F2 and the antagonism of IFN and the subsequently induced ISGs, we utilised a chicken IFN-2 promoter firefly luciferase reporter construct in DF-1 cells. The reporter was co-transfected with Poly I:C, which can induce the IFN- 2 promoter, a constitutively expressed Renilla reporter and PB1-F2 plasmids. We compared the ability of H5N1 5092 PB1-F2 with that of H9N2 UDL01 PB1-F2 and found that in line with our other results H5N1 5092 PB1-F2 was more potent at the antagonism of the chicken IFN- 2 promoter (Fig. 4(d)). In conjunction we utilised the chimeric PB1-F2 proteins containing the reciprocal C-terminus swaps, 5092:UDL01 and UDL01:5092 which show altered cellular localisations with respect to the mitochondria, than the parental PB1-F2 proteins. Our results demonstrated that possession of the H9N2 UDL01 C-terminus, which disrupted mitochondrial localisation, resulted in a reduced antagonism of the chicken IFN-2 promoter than those PB1-F2 proteins containing the H5N1 5092 C-terminus (Fig. 4(d)).

Co-localisation with the mitochondria did not correlate with enhanced PB1-F2 antagonism of an NFκB responsive promoter.

Influenza virus infection is known to activate NFκB transcription of cytokines involved in inflammation like IL-8 and IL-1b. In chickens infected by a H9N2 virus that possessed a full length PB1-F2 protein some of the transcripts for pro-inflammatory genes e.g. IL-6 and IL-1b were supressed compared to infection where the PB1-F2 was absent (Fig. 3(a)). To determine whether PB1-F2 from the avian influenza strains H9N2 UDL01 and

H5N1 5092 specifically antagonised NFκB activation we utilised a NFκB response element luciferase reporter construct in chicken DF-1 cells which was co-transfected with a constitutively active Renilla luciferase plasmid and PB1-F2 plasmids. Cells were stimulated by transfection with poly (Poly I:C) which activated NFκB leading to luciferase induction. Co-expression of H9N2 UDL01 PB1-F2 significantly inhibited the luciferase signal whereas co-expression of H5N1 5092 PB1-F2 did not, although there was the trend in multiple assays for the luciferase signal to be lower than no PB1-F2 expression (empty) (Fig. 5(a)). H9N2 UDL01 PB1-F2 inhibition of the NFκB response element was due to the inhibition of NFκB nuclear translocation (Supplementary Fig. 3).

We utilised our C-terminus swapped PB1-F2 constructs to determine the contribution of the C-terminus sequence, and by inference cellular localisation to the ability of PB1-F2 to antagonise NFκB activity. We found that both 5092:UDL01 and UDL01:5092 PB1-F2 proteins were able to significantly inhibit NFκB responsive promoter activity in this set up (Fig 5(a)). UDL01:5092 was only partially mitochondrial localised compared to H5N1 5092 which may explain this result.

Cytosolic localisation of PB1-F2 provides increased opportunity to directly interact with IKKβ but reduces PB1-F2 cellular stability.

We tested the ability of H5N1 5092 and H9N2 UDL01 PB1-F2 to interact with chicken IKKβ using co-immunoprecipitation in DF-1 cells (Fig. 5(b)). Both V5 tagged H9N2 UDL01 and H5N1 5092 PB1-F2 proteins were shown to co-precipitate with a FLAG tagged chicken IKKβ. The pulldown was more efficient with H9N2 UDL01 PB1-F2 than with H5N1 5092 PB1-F2 despite less H9N2 UDL01 PB1-F2 protein being present in the input

samples (Fig. 5(b)). We also saw, in DF-1 cells, chicken IKKβ localised more closely with H9N2 UDL01 PB1-F2 than that of H5N1 5092 (Fig. 5(c&d)). A general feature of our work with the H9N2 PB1-F2 protein was the instability of the protein in cells, we required the use of MG132, a well described proteasome inhibitor in order to obtain good visualisation in cells and by western blot. Despite the PB1-F2 proteins being cloned into the same plasmid background, with identical promoters and Kozak sequences, the H5N1 5092 PB1-F2 protein does not have the same instability seen with H9N2 UDL01 PB1-F2 (Fig. 6(a)). We hypothesised that the difference in cellular location of the two PB1-F2 proteins may result in different exposure to proteasomal mediated degradation, with interaction with MAVS at the mitochondria somehow shielding the H5N1 5092 PB1-F2 from degradation. To provide a quantified measure of protein stability in chicken DF-1 cells we performed a Cycloheximide chase assay and levels of PB1-F2 expression were determined post application of Cycloheximide by western blot. The H9N2 UDL01 PB1-F2 significantly degrades, from the levels detected at the point of cycloheximide application (Time = 0), within 30 minutes, whereas by 8 hours post Cycloheximide application, the H5N1 5092 PB1-F2 is still visible (Fig. 6(a-c)).

In Fig. 2 we demonstrated that swapping the H5N1 5092 C-terminus (5092:UDL01), or the 4 amino acids termed ‘4M’ for those in the H9N2 UDL01 (5092-4M) resulted in a disruption of the mitochondrial localisation of H5N1 5092, although the reciprocal mutations swaps did not completely relocalise H9N2 UDL01 PB1-F2 from the diffusely cytoplasm staining pattern to the equivalent level of H5N1 5092. We used the panel of mutant PB1-F2 proteins in the Cycloheximide chase assay and looked at the time-point 1 hour post Cycloheximide addition to transfected DF-1 cells. We found that disrupting

the mitochondrial localisation, (5092:UDL01 & 5092-4M) resulted in a significant difference in the stability of the PB1-F2 proteins (Fig. 6(b) & (c)).

Discussion

The capacity of IAV to encode a full length PB1-F2 is conserved in 93% of all avian host isolated IAVs compared to 43% and 48% from human and swine host isolates. We have previously demonstrated that the presence of a full length PB1-F2 in an avian IAV resulted in a longer virus shedding profile in chickens, increased viral tissue dissemination in infected birds and that these outcomes had a cumulative effect of prolonging the transmission window of the virus from an infected chicken to a naïve sentinel chicken [6]. The absence of a full length PB1-F2 also resulted in an increase in viral pathogenicity in chickens in both our previous study and that by Leymaire *et al* (2014) [6, 11]. PB1-F2 has been described previously to have cell type specific and viral strain specific activities. Here we show that PB1-F2 proteins from two avian IAVs of the subtypes H5N1 and H9N2 inhibit the production of type I IFN in chicken cells and can interact with chicken MAVS upstream of the type 1 interferon promoter (Fig. 3 & 4). In addition these two PB1-F2 proteins can antagonize NFκB activation and interact with chicken IKKβ (Fig. 5). PB1-F2 induced suppression of type 1 IFN and NFκB must occur *in vivo* in chickens since lower levels of ISG and pro-inflammation transcripts, which are stimulated by onward signaling from type 1 IFN induction and NFκB activation, were observed in nasal tissue from birds that were infected by H9N2 IAV containing an intact PB1-F2 protein. Specifically, the abundance of transcripts for the ISGs MX, OAS and STAT-1 and the pro-inflammatory associated cytokines IL-6 and IL-1β were all significantly reduced when infection was by

353 a virus possessing a full length PB1-F2 protein as compared to infection by an isogenic
354 virus that did not encode a functional PB1-F2. This suppression of ISGs and pro-
355 inflammation signals was also observed in a PB1-F2 dependent manner *in vitro* in primary
356 chicken fibroblasts and macrophages. Some differences in the magnitudes of the
357 transcript levels were observed between the CEFs and chicken BMDM upon infection by
358 isogenic viruses that differ only by the presence of PB1-F2, but this is likely due to different
359 sensitivities of fibroblast and myeloid cells to these induction signals since entry by the
360 viruses at high MOI appeared equal. There was little difference in the magnitude of
361 apoptosis caused by the individual viruses in the two different cell lines as measured
362 using a capsase3/7 activity reporter (data not shown). Leymarie *et al* (2014) also report
363 for another H5N1 influenza isolate that the presence of PB1-F2 suppresses innate
364 responsive transcripts during chicken infection [11].
365
366 There are clear differences in the components of the type 1 interferon pathway between
367 mammals and chickens, such as the lack of the pattern recognition receptor (PRR) RIG-
368 I and transcription factor IRF-3 in chickens. Instead the influenza pathogen associated
369 molecular pattern is recognized by the 'RIG-I like receptor' MDA5 in chicken cells which
370 then signals via chicken MAVS located at the mitochondria to the transcription factor IRF-
371 7 which induces the type 1 interferon promoter in the nucleus [27]. In this study we have
372 demonstrated for the first time an interaction between chicken MAVS, the mitochondrial
373 located interferon induction pathway adapter and PB1-F2 of two avian IAV strains.
374 Interaction of PB1-F2 with human MAVs has been previously demonstrated however
375 there is only 39% homology at the amino acid level between chicken and human MAVS
376 [19]. Our co-immunoprecipitation results suggested the interaction with chicken MAVS

was more efficient with the PB1-F2 from H5N1 5092 as compared to H9N2 UDL01 although both did display the interaction. In human 293T cells Varga et al (2012) showed that PB1-F2 of the vaccine strain A/PR/8/34 interacted with MAVS at the mitochondria and this resulted in a decreased mitochondrial membrane potential and antagonism of type 1 interferon production [19, 20]. It is likely that a similar mechanism is the cause of the type 1 interferon induction antagonism seen in chicken cells by PB1-F2 since we can demonstrate that interaction does occur with chicken MAVS and that the greater antagonism is seen by PB1-F2 proteins that co-localise at the mitochondria with MAVS, the H5N1 5092 PB1-F2 protein compared to the H9N2 UDL01 PB1-F2 (Fig. 1, Fig. 2 and Supplementary Fig.3).

Additionally for the first time we demonstrated interaction between PB1-F2 and chicken IKKβ. When NFκB is released from inhibition it translocates into the nucleus and acts as a transcription factor stimulating transcription of innate response genes, the phosphorylation action of the serine kinase, IKKβ on Iκb releases NFκB inhibition. It has been shown previously that PB1-F2 is able to interact directly with human IKKβ [28]. There is an 83% amino acid conservation between human and the chicken IKKβ homologue. We found that the H9N2 UDL01 PB1-F2 had a more efficient interaction with IKKβ than H5N1 5092. We hypothesize that interaction with chicken MAVS results in inhibition of onward interferon induction pathway simulation and is likely how PB1-F2 elicits an effect on ISG levels, similarly interaction of PB1-F2 with IKKβ may prevent phosphorylation of Iκb and thus inhibit translocation of NFκB to the nucleus resulting in inhibition of pro-inflammation cytokines. The variability in strength of interaction of the avian influenza virus PB1-F2 proteins with either chicken MAVS or chicken IKKβ

corresponded to the potency of the two PB1-F2 proteins to antagonize type I IFN induction and NFκB activation. More H5N1 5092 PB1-F2 was precipitated with chicken MAVS and it also had a greater ability to antagonize the type I IFN induction pathway as compared to H9N2 UDL01 PB1-F2. In contrast H9N2 UDL01 PB1-F2 had a bigger interaction with IKKβ and was able to significantly antagonize the activation of an NFκB dependent promoter in comparison to the H5N1 5092 PB1-F2 protein. The differences in antagonism potency correlated with the degree of PB1-F2 localisation to the mitochondria. Significant co-localisation with mitochondrial markers, including MAVS, was associated with enhanced antagonism of type I IFN production but reduced NFκB activation inhibition. Together this work suggests a mechanism by which PB1-F2 can interacts with chicken MAVS and chicken IKK-β to downregulate type 1 IFN and the downstream pro-inflammatory signals in infected cells in vivo, which results in a reduced pathogenicity and impaired viral clearance in chickens.

Cellular localization was established for a panel of avian influenza PB1-F2 proteins which clearly established two phenotypes; predominantly mitochondrial or predominantly cytoplasmic (Fig. 1). The two PB1-F2 proteins investigated here, H5N1 5092 and H9N2 UDL01 were representative of each group with H5N1 5092 being preferentially localized to the mitochondria, the location of chicken MAVS (Supplementary Fig. 2) and H9N2 UDL01 having a diffuse cytoplasmic localization that was the same as chicken IKKβ (Fig 5 (c)). It has previously been demonstrated that the C-terminus is responsible for mitochondrial localization of PB1-F2 in mammalian cells [23] and indeed when we swapped the C-terminus portions of the H5N1 5092 for that of H9N2 UDL01 PB1-F2 proteins we observed a re-localisation away from the mitochondria to the cytoplasm in

chicken fibroblast cells (Fig. 2). However a reciprocal swap only partially retargeted the PB1-F2 to the mitochondria, with statistical analysis by student T-test between the Pearson's localisation value for H5N1 5092 and UDL01:5092 indicating that they were still significantly different (p value = 0.008). This suggests features in the N-terminus of the H5N1 5092 PB1-F2 additionally contribute to mitochondrial localisation. By altering only 4 amino acids in the C-terminus of the H5N1 5092 to those found in the H9N2 UDL01 PB1-F2 protein (Q60R, L62H, S66N and T68I), our 5092-4M mutant, we disrupted the H5N1 5092 mitochondrial association (Fig. 2 (c)). A triple mutant H5N1 5092 PB1-F2 protein (L62H, S66N, T68I) where residues were changed to those found in the H9N2 UDL01 PB1-F2 as in the 5092-4M mutant did not result in significant retargeting of the H5N1 5092 PB1-F2 (data not shown). Cheng *et al* (2017) showed that the introduction of the motif I68, L69, V70 and F71 to H5N1 A/Hong Kong/156/97 relocated this PB1-F2 to the mitochondria in mammalian cells and replacement of this motif in the PB1-F2 of H1N1 A/Puerto Rico/8/34 removed mitochondria association [22]. We found no conservation of this motif in the PB1-F2 proteins we analysed for cellular localization. Similarly Chen *et al* (2010) demonstrated an enhancement of mitochondrial localization of H5N1 A/Hong Kong/156/97 PB1-F2 when two additional Leucine residues (Q69L and H75L) were introduced in the C-terminus [23]. Our analysis shown no correlation between the numbers of Leucine residues in the C-terminus of PB1-F2 and whether predominant mitochondrial localization occurs in chicken cells (Fig. 2(d)). Gibbs *et al* (2003) postulated the presence of an amphipathic helix and a short preceding hydrophobic patch in the C-terminus of PR8 PB1-F2 (aa 65 -87) and that this was responsible for the targeting of the protein to the mitochondria [24]. We found again no correspondence between this area of sequence, all the sequences we analysed regardless of observed cellular localisation

had a predicted helix structure and 4 out of the 5 basic residues observed in the PR8 amphipathic helix. The upstream hydrophobic residue patch was the same between viruses that had different cellular localisation.

PB1-F2 has a short half-life within cells and becomes ubiquitinated on conserved Lysine residues in the C-terminus as a post-translational modification [10]. Kosik *et al* (2015) demonstrated that mutation of the C-terminal Lysine residues at positions 73, 78 and 85 to Arginines reduced ubiquitination and increased the stability of PB1-F2 in mammalian cells. We found that H9N2 UDL01 had one fewer Lysine residues in the C-terminus sequence compared to H5N1 5092 (Fig. 2(d)) but when the stability of both the H9N2 UDL01 and H5N1 5092 PB1-F2 proteins and the derived C-terminal altered mutants in chicken cells was assessed, we found that cellular localization, not the presence of Lysines in the C-terminal sequence, correlated with protein stability. H5N1 5092 had a strong co-localisation with the mitochondria and was the PB1-F2 protein that was most stable in chicken DF-1 cells. In contrast disruption of the H5N1 5092 mitochondrial localization via C-terminal (5092:UDL01) or 4 residue swap (5092-4M) with the H9N2 UDL01 PB1-F2 resulted in significant degradation of the PB1-F2 protein by 1 hours post cycloheximide addition. We suggest therefore, that PB1-F2 proteins that are predominantly targeted to the mitochondria are protected from ubiquitin directed proteosomal degradation compared to PB1-F2 proteins that have a diffuse cytoplasmic localization. Indeed studies by others also support this hypothesis, Cheng *et al* (2017) demonstrate that the predominantly mitochondria located PB1-F2 of A/Puerto Rico/8/34 has a significantly higher half-life in HeLa cells compared to the PB1-F2 from A/Hong Kong/156/97 which was cytoplasmic in localization and this finding was also observed by

Kosik *et al* (2015) for the same strains in 293T cells [10, 22]. Chen *et al* (2010) showed that a H1N1 A/Taiwan/3355/1997 PB1-F2 which localized to the mitochondria had the same stability in 293T cells as the A/Puerto Rico/8/34 PB1-F2 [23]. PB1-F2 has been shown to have dramatically differing secondary structure dependent upon sequence and the environment in which the proteins reside [29, 30]. In aqueous solution they are disordered and in the presence of membranes can structured fibre which can disrupt those membranes [8]. The differing predominant localisations of the H5N1 5092 and H9N2 UDL01 PB1-F2 viruses could influence the protein structure in infected cells and consequently their functionality.

Our results suggest that the PB1-F2 protein can operate at different points within innate immune signaling pathways in a strain-specific manner reminiscent of the influenza NS-1 protein and that localization of PB1-F2 in the cell a driving factor of the protein's functionality. PB1-F2 is encoded from the +1 reading frame of the functionally important RNA dependent RNA polymerase, PB1. Analyses indicate that the first two positions in the codon of PB1-F2 varied more than position three which is in line with +1 translation frame from PB1 and this contributes to the high non-synonymous to synonymous ratio found for PB1-F2 proteins [31, 32]. The fact that PB1-F2 proteins with different amino acid sequence can use varying mechanisms to achieve the same innate pathway antagonism indicates that this function at least in avian cells is important. Whether evolution of the other viral proteins over-rides selection towards one mechanism or another is yet to be determined.

Materials and Methods

Ethics Statement

All animal work was approved and regulated by the UK government Home Office under the project license (PPL 30/2952). All personnel involved in the procedures were licensed by the UK Home Office. Euthanasia of chickens was carried out by intravenous administration of sodium pentobarbital and confirmed through cervical dislocation.

Cells

MDCK, 293T and Chicken fibroblast Doug Foster 1 (DF-1) cells were grown in Complete Media (DMEM (Gibco-Invitrogen, Inc.) supplemented with 10% foetal bovine serum (FBS) (Biosera, Inc.), 1% penicillin/streptomycin (Sigma-Aldrich) and 1% non-essential aa (Sigma-Aldrich)) and maintained at 37°C in 5% CO2.

Primary chicken embryo fibroblasts (CEFs) were produced from 10-day-old Rhode Island Red chicken embryos from specific pathogen free (SPF) hens. Embryos were homogenized and trypsinised with 0.25% Trypsin-EDTA solution (Sigma-Aldrich). The homogenate re-suspended in Complete Media and passed through a Falcon Cell Strainer (Fisher) before being seeded on to plates for experimentation. Influenza infections were conducted in Eagle's Minimum Essential Medium (EMEM) supplemented with 0.35% Bovine Serum Albumin (BSA) (Sigma-Aldrich), 1% Penicillin-Streptomycin and 0.25 µg/ml TPCK treated trypsin.

Primary chicken bone marrow derived macrophage cells (ckBMDM) were produced from male 3-week-old Rhode Island Red chickens from a SPF flock. Femurs were extracted,

and the marrow flushed and liberated with phosphate-buffered saline (PBS). The cells were homogenized, passed through a Falcon Cell Strainer and then isolated via centrifugation on Histopaque 1083 (Sigma-Aldrich). The cells were washed and resuspended in Roswell Park Memorial Institute medium-1640 (RPMI-1640) Medium (Invitrogen) supplemented with 5 % FBS and 5 % chicken serum (Pirbright), 2.95 g/L TBP (Sigma-Aldrich), 1 mM Sodium Pyruvate (Sigma-Aldrich) and 1% Penicillin-Streptomycin and seeded onto plates for experimentation. BMDMs were stimulated to differentiate by addition of 10 ng/ml of chicken colony-stimulating factor 1 (cCSF-1) for 5 days (The Roslin Institute). Influenza infections were conducted in the same media without serum.

Primary chicken kidney cells (CKCs) were produced from 2- 3-week-old Rhode Island Red chickens from a SPF flock. Kidneys were extracted, homogenized and trypsinised with 0.25% Trypsin-EDTA solution (Sigma). The homogenate was washed and re-suspended in EMEM (Invitrogen) supplemented with 10 % FBS (Sigma), 2.95 g/L tryptose phosphate broth (TPB) (Sigma), 10 mM HEPES (Sigma) and 1x Penicillin-Streptomycin (Sigma). The homogenate was passed through a Falcon Cell Strainer (Fisher) and seeded on to plates for experimentation. Influenza infections were conducted in the same medium without serum.

Viruses

Recombinant A/chicken/Pakistan/UDL01/08 H9N2 virus (H9N2 UDL01) and a reassortant H5N1 5092 influenza virus where the NS, NP, PA, PB1 and PB2 viral genetic segments were from A/Turkey/England/5092/91 H5N1 virus and the HA, NA and M viral genetic segments were from the vaccine strain A/PR/8/34 H1N1 virus were generated using reverse genetics. Both H9N2 UDL01 PB1-F2-KO and H5N1 5091 PB1-F2-KO viruses

were generated by introduction of a stop codon at aa position 12 in the PB1-F2 reading frame, this was constructed by site directed mutagenesis in the PB1 genetic segment prior to reverse genetics rescue of virus. Reverse genetics virus rescue was performed by transfection of Human Embryonic Kidney (HEK) 293T cells (ATCC) and co-culture in Madin-Darby Canine Kidney (MDCK) cells (ATCC) with addition of 2µg/ml of TPCK treated Trypsin (Sigma-Aldrich).

Expression Plasmids

The open reading frame (ORF) of PB1-F2 from the listed avian influenza viruses; H5N1 50-92 (A/Turkey/England/5092/91), H3N8a (A/mallard/Alb/156/2001), H10N7 (A/duck/Italy/1398/V06), H9N2 UDL01 (A/chicken/Pakistan/UDL01/08), H8N4 (A/mallard/Alb/194/92), H11N9 (A/duck/Italy/6103/V07), H3N8b (A/duck/Italy/3139/V06), H6N2 (A/duck/Italy/2253/V06), were cloned into the eukaryotic expression vector pCAGGs with an N-terminal V5 tag placed in frame. H5N1 5092 and H9N2 UDL01 PB1-F2 protein were also cloned in the pCAGGs expression vector with an in frame FLAG tag at the N-terminus. These PB1-F2 expression plasmids along with a pCAGGs vector containing eGFP were used in confocal microscopy and co-immunoprecipitation experiments. Full-length cDNA clones of chicken MAVS and chicken IKKβ were generated from DF1 cells treated with chicken IFN (1000 U/ml) overnight and cloned into the expression plasmid pEF.pLink2 [33].

Co-localisation studies in DF-1 cells

DF-1 cells were grown on coverslips before being transfected with the appropriate expression plasmids. 5µM MG132 (Sigma-Aldrich) was applied to the cells 4 hours post

transfection. At 12 hours post transfection cells were fixed in 10% formalin (Sigma-Aldrich) then permeabilised in 0.1% Triton X-100 (Sigma-Aldrich) in PBS. For mitochondrial staining, cells were incubated in serum free DMEM containing 200 nM of MitoTracker CMX-Ros (Thermo-Fisher) prior to fixation. Nuclei were stained with 0.2 µg/ml of DAPI (4',6-diamidino-2-phenylindole) (Sigma-Aldrich) in dH_2O. Proteins tagged with V5 or FLAG, were stained using a 1:1000 dilution of either Rabbit αV5 (GeneTex), mouse anti-V5 (SourceBioScience) or Mouse αFLAG (M2, Sigma) or rabbit anti-FLAG (GeneScript) and by using Goat anti-Mouse IgG (H+L) Alexa Flour 488 or 568 and Goat anti-Rabbit IgG (H+L) Alexa Flour 488 or 568 (Thermo-Fisher) as appropriate. Confocal microscopy images were acquired sequentially using a TCS SP5 Confocal microscope (Leica) and 100x objective lens using mineral oil immersion and analysed using Leica Application Suite X (Lecia). The transect analysis was based on the published method by Horner *et al* (2011), different channels from the same image were overlaid using ImageJ (National Institutes for Health, NIH) [34]. Three, 5 pixel wide lines per image were randomly drawn in the MitoTracker or MAVS channel, transecting the area of interest. Pixel intensities along transects were obtained for both channels of interest and displayed graphically. The three transects were individually compared using Pearson's correlation coefficient and the average coefficient obtained per image. Graphical representations of the averaged Pearson's R-values are for at least 10 separate images from two independent experiments. For nuclear vs cytoplasmic localisations, multiple images were acquired as above from random fields. The intensity of straining in the nuclear vs cytoplasmic proportions was acquired using these images and Cell Profiler (Broad Institute) according to a published method [35].

Chicken gene transcript quantification

Nasal tissues were dissected, weighed and added to 700 µl of TRIzol Reagent (Life Technologies). Tissue was homogenised with a 5 mm Stainless Steel Bead (Qiagen) for 4 min at 20 Hz using a TissueLyser II (Qiagen). RNA was then extracted from centrifuge clarified homogenate via chloroform and ethanol precipitation. RNA was isolated from cells using a silica-membrane based RNeasy Mini Kit (Qiagen) according to manufacturer's instructions. Genomic DNA was eliminated using RNase-Free DNase On-Column Digestion (Qiagen). For subsequent analysis of host transcripts by RT-qPCR, cDNA synthesis was performed using Random Primers (Thermo-Fisher) and SuperScript III Reverse Transcriptase (Invitrogen). All quantitative PCR (qPCR) was performed using a 7500 Fast & Real-Time PCR System (Applied Biosystems). 20 µl of either TaqMan Universal PCR Master Mix or Power SYBR Green Master Mix were used with 2 µl of cDNA according to manufacturer's instructions with primer and probe sets defined the table below, Table 2. Gene expression data was normalized against a stable reference gene and compared against the mock controls using the 2-ΔΔCt method [36]. Reference genes, RDPLO-1 and RSAD were selected from previous data using GeNorm Reference Gene Selection Software (GeNorm) analysis of multiple reference genes on independent samples under identical conditions (Whitehead *et al*, 2017 under review).

Viral RNA quantification

Quantification of vRNA was performed as previously described [6]. Briefly, a SuperScript III One-Step reverse transcription-PCR (RT-PCR) System with Platinum Taq DNA

Polymerase kit (Invitrogen) was performed according to manufactures instructions using a 7500 Fast & Real-Time PCR System (Applied Biosystems). Primers and a Taqman probe, specific for a conserved region of the Influenza A Matrix gene were used as previously published (Spackman et al., 2001). Cycling conditions were; 50 °C for 5 min, 95 °C for 2 min and then 40 cycles of 95 °C for 3 s and 60 °C for 30 s. A T7 transcribed RNA standard of the M gene from A/PR 8/34 (H1N1) was included in each assay to generate a standard curve. CT values were extrapolated against this curve and the results were expressed as copy numbers of influenza M gene.

Co-immunoprecipitation of PB1-F2 and ck MAVs or ck IKKβ

Chicken MAVS-V5 or IKKβ-FLAG expression plasmids were co-transfected into DF-1 cells along with PB1-F2 containing a FLAG or V5 tag as appropriate, using lipofectamine 2000 according to manufactures instructions. After incubation for 24 h after transfection, cells were lysed in Pierce immuoprecipitation Lysis Buffer (Thermo-Fisher) and then processed immediately. The lysates were precleared by adding 0.5 mg/ml of Pierce Protein G Magnetic Beads (Thermo-Fisher) and a 12-Tube Magnetic rack (Qiagen). The samples were incubated overnight at 4 °C with 10 µg/ml of primary antibody (mouse anti-FLAG (Sigma M2) or rabbit anti-V5 (Genetex) antibody, then incubated at 4 °C for 6 h with 0.5 mg/ml of magnetic beads. The beads were magnetically isolated and washed three times in Pierce IP Lysis Buffer (Thermo-Fisher). Beads were then boiled in SDS-loading dye for 10 min and used for western blot analysis.

VSV-GFP Interferon bioassay.

631 The supernatants from three independent experiments involving cells infected with each
632 indicated influenza virus at an MOI of 3 were heated at 60 °C for 30 min to inactivate
633 influenza virus. This was confirmed thorough performing in-cell enzyme-linked
634 immunosorbent assay (ELISA) for influenza nucleoprotein. In technical triplicate, the
635 supernatants were 2-fold serially diluted in Complete Media on DF-1 cells (4 x 10^4
636 cells/well) in a 96-well opaque white plate (Pierce) and incubated for 12 h. Cells were
637 infected with GFP tagged Vesicular Stomatitis Virus (VSV-GFP)) [37] at a multiplicity of
638 infection (MOI) of 3 in Opti-MEM with no phenol red (Thermo). 12 hours post infection
639 (hpi), media was removed and GFP fluorescence was measured using a GloMax Multi
640 plate reader fluorescence module (Promega). SF9 produced chicken interferon-β was
641 used as a positive control (The Pirbright Institute). No VSV-GFP virus was used to
642 establish background fluorescence and media only incubations were used to establish
643 maximum fluorescence. The percentage antiviral effect was then calculate dusing the
644 following formula and displayed graphically.

645 $$\%\ Antiviral\ Effect = \frac{(sample\ fluor\ - background\ fluor)\ X\ 100}{max\ fluor - background\ fluor} - 100$$

646 **Luciferase reporter assays.**

647 For assaying interferon modulation a pGL3 Luciferase (luc) reporter vector was used
648 containing the promoter regions from chicken IFN-2 upstream of a Firefly luc gene. For
649 assaying NF-κB activity, a similar reporter vector was used containing six tandem repeats
650 of the NF-κB consensus binding sequence (5'-GGGACTTTCC-3') upstream of a
651 thymidine kinase (TK) minimal promoter. In triplicate, cells were transfected according
652 with 100 ng of Renilla luc pCAGGs expression plasmid, 500 ng chIFN-2-, chMX- or NF-
653 κB Luciferase reporter plasmids and 2μg PB1-F2 protein expression plasmids. For assays

involving polyinosinic:polycytidylic acid (poly (I:C)) stimulation, 6 hpt cells were re-transfected with 0.25µg poly (I:C) (Sigma). After the experimental time point was reached, cells were lysed and read using the Stop and Glo reagents (Promega). Each individual Firefly and Renilla value was checked for consistency, and then the Firefly luciferase signals were normalized to Renilla signals.

Cycloheximide chase assay

DF1s were transfected with 250ng/ul of the appropriate V5-PB1-F2 or GFP plasmid. 24hrs post transfection, cells were treated with 100ug/ml Cycloheximide (Sigma). Samples were collected at appropriate time points by washing with PBS and lysing with Laemmli buffer. Samples were visualised on western blots using mouse anti-V5 antibody (abcam) and IRDye donkey anti mouse 800 nm (LiCor). Actin was used as a loading control and visualised using mouse anti actin antibody (abcam) with IRDye donkey anti mouse 800 nm (LiCor). GFP was used as a stable protein control. Bands were quantified using ImageJ (NIH) and PB1-F2 normalised to actin loading control.

Viral polymerase activity assay

In triplicate, DF-1 cells were transfected with 20 ng of PA, 160 ng of NP, 80 ng of each PB1 and PB2 pCAGGs expression plasmids. Transfection reactions also included 250 ng of chicken specific viral RNA-dependent-RNA-polymerase Firefly luciferase reporter (described previously [38]) and 100 ng of a Renilla Luciferase pCAGGs expression plasmid. Cells were incubated for 24 hours at either 37°C or 41°C before being lysed in 100 µl of 1 X passive lysis buffer (Promega). Plates were frozen for 30 min at -80 °C and defrosted before reading. 10 µl of lysate was loaded onto a 96-well opaque

white plate (Pierce) and analysed on a GloMax Multi plate reader (Promega) with 50 µl of LARII and Stop and Glo reagents (Promega). Each individual Firefly and Renilla value was checked for consistency, and then the Firefly luciferase signals were normalized to Renilla signals.

Viral growth curves

In triplicate, in 6 well plates, chicken kidney cells were infected with a virus MOI of 0.0001 1 h at 37°C. The cells were washed with PBS and incubated at 37 °C with 2 ml of appropriate media containing no serum. 500 µl of supernatant were taken at the indicated time points after infection, replenished, and samples were stored at -80 °C. All samples were titrated via plaque assay on MDCK cells including the input.

Funding Information

This work described herein was funded by The Pirbright Institute studentship grant BBS/E/00001759, BBSRC ISP Grant BBS/E/I/00001650, BBS/E/I/00007034 & BBS/E/I/00007038. The funders had no role in study design, data collection, data interpretation, or the decision to submit the work for publication.

Acknowledgments

We would like to acknowledge members of the Influenza Virus and Avian Influenza groups at The Pirbright Institute who supported this work; Dr Dagmara Bialy, Dr Thomas Peacock, Dr Jean-Remy Sadeyen, Dr Pengxiang Chang, Dr Sushant Bhat, Anabel Clements and Joshua Sealy. We thank Dr Muhammed Munir at The University of Lancaster, UK for the kind gift of the VSV-GFP virus for use in the IFN bioassay. PB1-F2

was cloned from viruses (A/mallard/Alb/156/2001 and A/mallard/Alberta/194/92) kindly provided by Professor Robert Webster and Dr Scott Krauss of the St Judes Children's Research Hospital, Memphis, USA. PB1-F2 was cloned from viruses (A/duck/Italy/3139/V06, A/duck/Italy/2253/V06, A/duck/Italy1398/V06, A/duck/Italy/6103/V07) kindly provided by Professor Ilaria Capua, Dr Isabella Monne and Dr Calogero Terregino of the Instituto Zooprofilattico Sperimentalle delle Venezie, Italy.

Author contributions

The work was conceptualised by HS, JJ, MI, and WB. Experimental work was executed by JJ, HS, CR and NS. The Manuscript was written by JJ and HS and edited by all authors. PD and SG provided resources and intellectual input into the project.

Conflicts of Interest

The authors declare that there are no conflicts of interest.

References

1. Basuno E, Yusdja Y, Ilham N. Socio-economic impacts of avian influenza outbreaks on small-scale producers in Indonesia. Transbound Emerg Dis 2010;57(1-2):7-10.

2. Govindaraj G, Sridevi R, Nandakumar SN, Vineet R, Rajeev P et al. Economic impacts of avian influenza outbreaks in Kerala, India. Transbound Emerg Dis 2018;65(2):e361-e372.

716 3. Qi X, Jiang D, Wang H, Zhuang D, Ma J et al. Calculating the burden of disease of
717 avian-origin H7N9 infections in China. BMJ Open 2014;4(1):e004189.

718 4. Vasin AV, Temkina OA, Egorov VV, Klotchenko SA, Plotnikova MA et al. Molecular
719 mechanisms enhancing the proteome of influenza A viruses: an overview of recently
720 discovered proteins. Virus research 2014;185:53-63.

721 5. Chen W, Calvo PA, Malide D, Gibbs J, Schubert U et al. A novel influenza A virus
722 mitochondrial protein that induces cell death. Nature medicine 2001;7(12):1306-1312.

723 6. James J, Howard W, Iqbal M, Nair V, Barclay WS et al. Influenza A Virus PB1-F2
724 Protein Prolongs Viral Shedding in Chickens Lengthening the Transmission Window. The
725 Journal of general virology 2016.

726 7. Zell R, Krumbholz A, Eitner A, Krieg R, Halbhuber KJ et al. Prevalence of PB1-F2
727 of influenza A viruses. The Journal of general virology 2007;88(Pt 2):536-546.

728 8. Kamal RP, Alymova IV, York IA. Evolution and Virulence of Influenza A Virus
729 Protein PB1-F2. Int J Mol Sci 2017;19(1).

730 9. Klemm C, Boergeling Y, Ludwig S, Ehrhardt C. Immunomodulatory Nonstructural
731 Proteins of Influenza A Viruses. Trends Microbiol 2018.

732 10. Kosik I, Praznovska M, Kosikova M, Bobisova Z, Holly J et al. The
733 ubiquitination of the influenza A virus PB1-F2 protein is crucial for its biological function.
734 PloS one 2015;10(4):e0118477.

11. Leymarie O, Embury-Hyatt C, Chevalier C, Jouneau L, Moroldo M et al. PB1-F2 attenuates virulence of highly pathogenic avian H5N1 influenza virus in chickens. PloS one 2014;9(6):e100679.

12. de Jong MD, Simmons CP, Thanh TT, Hien VM, Smith GJ et al. Fatal outcome of human influenza A (H5N1) is associated with high viral load and hypercytokinemia. Nature medicine 2006;12(10):1203-1207.

13. Writing Committee of the Second World Health Organization Consultation on Clinical Aspects of Human Infection with Avian Influenza AV, Abdel-Ghafar AN, Chotpitayasunondh T, Gao Z, Hayden FG et al. Update on avian influenza A (H5N1) virus infection in humans. The New England journal of medicine 2008;358(3):261-273.

14. Chang P, Kuchipudi SV, Mellits KH, Sebastian S, James J et al. Early apoptosis of porcine alveolar macrophages limits avian influenza virus replication and pro-inflammatory dysregulation. Sci Rep 2015;5:17999.

15. Dudek SE, Wixler L, Nordhoff C, Nordmann A, Anhlan D et al. The influenza virus PB1-F2 protein has interferon antagonistic activity. Biol Chem 2011;392(12):1135-1144.

16. Leymarie O, Meyer L, Tafforeau L, Lotteau V, Costa BD et al. Influenza virus protein PB1-F2 interacts with CALCOCO2 (NDP52) to modulate innate immune response. The Journal of general virology 2017;98(6):1196-1208.

17. Yoshizumi T, Ichinohe T, Sasaki O, Otera H, Kawabata S et al. Influenza A virus protein PB1-F2 translocates into mitochondria via Tom40 channels and impairs innate immunity. Nat Commun 2014;5:4713.

18. Conenello GM, Tisoncik JR, Rosenzweig E, Varga ZT, Palese P et al. A single N66S mutation in the PB1-F2 protein of influenza A virus increases virulence by inhibiting the early interferon response in vivo. Journal of virology 2011;85(2):652-662.

19. Varga ZT, Grant A, Manicassamy B, Palese P. Influenza virus protein PB1-F2 inhibits the induction of type I interferon by binding to MAVS and decreasing mitochondrial membrane potential. Journal of virology 2012;86(16):8359-8366.

20. Varga ZT, Ramos I, Hai R, Schmolke M, Garcia-Sastre A et al. The influenza virus protein PB1-F2 inhibits the induction of type I interferon at the level of the MAVS adaptor protein. PLoS pathogens 2011;7(6):e1002067.

21. Chen S, Cheng A, Wang M. Innate sensing of viruses by pattern recognition receptors in birds. Vet Res 2013;44:82.

22. Cheng YY, Yang SR, Wang YT, Lin YH, Chen CJ. Amino Acid Residues 68-71 Contribute to Influenza A Virus PB1-F2 Protein Stability and Functions. Front Microbiol 2017;8:692.

23. Chen CJ, Chen GW, Wang CH, Huang CH, Wang YC et al. Differential localization and function of PB1-F2 derived from different strains of influenza A virus. Journal of virology 2010;84(19):10051-10062.

774 24. Gibbs JS, Malide D, Hornung F, Bennink JR, Yewdell JW. The influenza A
775 virus PB1-F2 protein targets the inner mitochondrial membrane via a predicted basic
776 amphipathic helix that disrupts mitochondrial function. Journal of virology
777 2003;77(13):7214-7224.

778 25. Yamada H, Chounan R, Higashi Y, Kurihara N, Kido H. Mitochondrial
779 targeting sequence of the influenza A virus PB1-F2 protein and its function in
780 mitochondria. FEBS Lett 2004;578(3):331-336.

781 26. Reuter A, Soubies S, Hartle S, Schusser B, Kaspers B et al. Antiviral activity
782 of lambda interferon in chickens. Journal of virology 2014;88(5):2835-2843.

783 27. Liniger M, Summerfield A, Zimmer G, McCullough KC, Ruggli N. Chicken
784 cells sense influenza A virus infection through MDA5 and CARDIF signaling involving
785 LGP2. Journal of virology 2012;86(2):705-717.

786 28. Reis AL, McCauley JW. The influenza virus protein PB1-F2 interacts with
787 IKKbeta and modulates NF-kappaB signalling. PloS one 2013;8(5):e63852.

788 29. Miodek A, Sauriat-Dorizon H, Chevalier C, Delmas B, Vidic J et al. Direct
789 electrochemical detection of PB1-F2 protein of influenza A virus in infected cells. Biosens
790 Bioelectron 2014;59:6-13.

791 30. Miodek A, Vidic J, Sauriat-Dorizon H, Richard CA, Le Goffic R et al.
792 Electrochemical detection of the oligomerization of PB1-F2 influenza A virus protein in
793 infected cells. Anal Chem 2014;86(18):9098-9105.

794 31. Wei P, Li W, Zi H, Cunningham M, Guo Y et al. Epidemiological and
795 molecular characteristics of the PB1-F2 proteins in H7N9 influenza viruses, Jiangsu.
796 Biomed Res Int 2015;2015:804731.

797 32. Holmes EC, Lipman DJ, Zamarin D, Yewdell JW. Comment on "Large-scale
798 sequence analysis of avian influenza isolates". Science 2006;313(5793):1573; author
799 reply 1573.

800 33. Marais R, Light Y, Paterson HF, Marshall CJ. Ras recruits Raf-1 to the
801 plasma membrane for activation by tyrosine phosphorylation. EMBO J 1995;14(13):3136-
802 3145.

803 34. Horner SM, Liu HM, Park HS, Briley J, Gale M, Jr. Mitochondrial-associated
804 endoplasmic reticulum membranes (MAM) form innate immune synapses and are
805 targeted by hepatitis C virus. Proceedings of the National Academy of Sciences of the
806 United States of America 2011;108(35):14590-14595.

807 35. Carpenter AE, Jones TR, Lamprecht MR, Clarke C, Kang IH et al.
808 CellProfiler: image analysis software for identifying and quantifying cell phenotypes.
809 Genome Biol 2006;7(10):R100.

810 36. Pfaffl MW. A new mathematical model for relative quantification in real-time
811 RT-PCR. Nucleic Acids Res 2001;29(9):e45.

812 37. Berger Rentsch M, Zimmer G. A vesicular stomatitis virus replicon-based
813 bioassay for the rapid and sensitive determination of multi-species type I interferon. PLoS
814 One 2011;6(10):e25858.

38. Moncorge O, Long JS, Cauldwell AV, Zhou H, Lycett SJ et al. Investigation of influenza virus polymerase activity in pig cells. Journal of virology 2013;87(1):384-394.

39. Giotis ES, Robey RC, Skinner NG, Tomlinson CD, Goodbourn S et al. Chicken interferome: avian interferon-stimulated genes identified by microarray and RNA-seq of primary chick embryo fibroblasts treated with a chicken type I interferon (IFN-alpha). Vet Res 2016;47(1):75.

Tables

Table 1. Subtypes of avian influenza virus from which the PB1-F2 proteins were extracted for study.

Virus short name	Viral strain	Length of PB1-F2 protein (aa)
H3N8a	A/mallard/Alb/156/2001	90
H3N8b	A/duck/Italy/3139/V06	90
H5N1 5092	A/Turkey/England/5092/91	90
H6N2	A/duck/Italy/2253/V06	90
H8N4	A/mallard/Alb/194/92	90
H9N2 UDL01	A/chicken/Pakistan/UDL01/08	90
H10N7	A/duck/Italy/1398/V06	90
H11N9	A/duck/Italy/6103/V07	90

Table 2. qPCR and RT-qPCR oligonucleotides [39]

Gene	***Fwd (5' to 3')***	***Rev (5' to 3')***	***Probe (5' to 3')***
IFN-λ	*GGCCTTCCTTACCC AAGTCC*	*CCAGTGCCTC AGTTTCCCAG*	*SYBR Green*
OAS	*AAGAACTGGGACTT GGTGGC*	*CCTTCAGCTC CCAGACTGTG*	*SYBR Green*

RSAD-2	*GGACAAGGACGAGACAGTTCC*	*TCCCGCCTCCTTAAGCATTG*	*SYBR Green*
STAT-1	*ACTGCATGCATTGGTGGCCCA*	*GCTGACGAACTTGCTGCAGGC*	*SYBR Green*
IFN-1	*GACAGCCAACGCCAAGC*	*GTCGCTGCTGTCCAAGCATT*	*(FAM)CTCAACCGGATCCACCGCTACACC(TAMRA)*
IFN-2	*CCTCCAACACCTCTTCAACATG*	*TGGCGTGCGGTCAAT*	*(FAM)TTAGCAGCCCACACACTCCAAAACACTG(TAMRA)*
IFN-γ	*GTGAAGAAGGTGAAAGATATCATGGA*	*GCTTTGCGCTGGATTCTCA*	*(FAM)TGGCCAAGCTCCCGATGAACGA(TAMRA)*
IL-1β	*GCTCTACATGTCGTGTGTGATGAG*	*TGTCGATGTCCCGCATGA*	*(FAM)CCACACTGCAGCTGGAGGAAGCC(TAMRA)*
IL-6	*AACATGCGTCAGCTCCTGAAT*	*TCTGCTAGGAACTTCTCCATTGAA*	*(FAM)AGCAGCACCTCCCTCAAGGCACC(TAMRA)*
IL-8	*GCCCTCCTCCTGGTTTCAG*	*TGGCACCGCAGCTCATT*	*(FAM)TCTTTACCAGCGTCCTACCTTGCGACA(TAMRA)*
IL-10	*CATGCTGCTGGGCCTGAA*	*CGTCTCCTTGATCTGCTTGATG*	*(FAM)CGACGATGCGGCGCTGTCA(TAMRA)*

MX	*CACTGCAACAAGCAAAGAAGGA*	*TGATCAACCCCACAAGGAAAA*	*(FAM)ACAAAGCACACACCCAACTGTCAGCG(TAMRA)*
RDLPO-1	*TTGGGCATCACCACAAAGATT*	*CCCACTTGTCTCCGGTCTTAA*	*(FAM)CATCACTCAGAATTTCAATGGTCCCTCGGG(TAMRA)*
RPL13	*TCGTGCTGGCAGGATTC*	*TCGTCCGAGCAAACCTTTTG*	*(FAM)TAATGCCCGCCAGTTTAAGCTCTTCTAGGC(TAMRA)*

Figure Legends

Fig. 1. PB1-F2 protein from avian influenza viruses have different subcellular locations in chicken cells. PB1-F2 proteins from a range of avian influenza subtypes were cloned into expression plasmids. DF-1 cells were transfected with V5-PB1-F2 expression plasmids and 12 hours post transfection stained with MitoTracker Red CMXRos (Mitochondria [Red]). The cells were subsequently fixed and immunostained with an anti-V5 antibody (PB1-F2 [Green]) and the nuclei stained with DAPI (Nucleus [Blue]). Lines were drawn transecting objects in the 'Red' channel (displayed as white lines) and pixel intensities along these transects for both the 'red' and 'green' channels were displayed graphically. Pearson's correlation coefficients for of transects were calculated and the R^2 values were displayed. Displayed are representative of these lines which were drawn randomly at three locations per image.

Fig. 2. PB1-F2 protein localisation to the mitochondria in chicken cells was mapped to residues in the C-terminus of PB1-F2. (a) Schematic of the amino acid differences between H5N1 5092 (Red) and H9N2 UDL01 (Blue) PB1-F2 proteins. Chimeric proteins were constructed that had the entire C-terminal portions (5092:UDL01 and UDL01:5092) or 4 residues; 60, 62, 66 and 68 (5092-4M and UDL01-4M) swapped between the H5N1 5092 and H9N2 UDL01 strains. (b) & (c). DF-1 cells were transfected with the wild type V5- PB1-F2 proteins or the V5-PB1-F2 chimeras and stained to indicate the co-localisation between V5-PB1-F2 (Green) and mitochondria (Red). Nuclear staining is indicated by DAPI staining (Blue). Transects (white lines) drawn in both the mitochondria and PB1-F2 channel were compared via a Pearson correlation coefficient. In (b) the Pearson's correlation coefficient (R^2) values from ten cells for each PB1-F2 construct were averaged and plotted. 1 way ANOVA was used to determine if significant difference in the correlations existed. ****= P< 0.0005, (ns = not significant). (d). The C-terminal sequences (aa 45-90) of the PB1-F2 proteins analysed in Fig. 1 in addition to as the well characterized H1N1 (A/PR/8/34) and H5N1 (A/HK/196/97) were aligned. Differences at the 4M mutations (aa 60, 62, 66 and 68) are highlighted as is mitochondrial localization (Mitochondrial = Y, Cytoplasmic = N) and the number of Leucine residues in the C-terminal fragment (Leucines).

Fig. 3. In vivo and in vitro, PB1-F2 suppresses chicken interferon stimulated gene and pro-inflammatory gene transcripts. Total RNA was isolated from the chicken substrates detailed. The RNA was reverse transcribed and used to quantify chicken host response genes via qPCR. Ct values were compared to those of the reference gene RPLPO1 and quantified using the ΔΔCt method of quantification. The means +/- SD are

862 shown. Multiple student t-tests were performed to compare between WT and KO means
863 and the Holm-Sidak correction for multiple comparisons was applied. * indicates P≤0.05,
864 ** indicates P≤0.01. (a) Nasal tissue taken from six chickens infected with influenza virus
865 possessing a full length PB1-F2 protein (H9N2 UDL01) or a point mutation abrogating
866 PB1-F2 expression (H9N2 UDL01 KO) at day 2 or day 5 post infection. (b) Primary
867 chicken embryonic fibroblast (CEF) cells or (c) chicken bone marrow derived macrophage
868 (BMDM) cells infected with an MOI of 3 of H9N2 UDL01 or H5N1 5092 viruses that have
869 a full length PB1-F2 or a knock-out PB1-F2 (KO). Cells were lysed at 8 hours post
870 infection for RNA isolation and repeated in three independent experiments. Supernatants
871 from CEF cells (d) or from chicken BMDM cells (e) infected with H9N2 UDL01 or H5N1
872 5092 viruses that have a full length PB1-F2 or a knock-out PB1-F2 (KO) were incubated
873 on MDCK cells for 12 hours and assayed for the presence of IAV nucleoprotein (NP) with
874 a mouse anti NP antibody and anti-mouse IRDye 800CW antibody (LI-COR) before being
875 visualized by the Odyssey Imaging System (LI-COR).

876 **Fig. 4. Co-localisation of PB1-F2 with mitochondria increases the antagonism of**
877 **the IFN2 promoter.** (a) DF-1 cells were transfected with over-expression plasmids for
878 the wild type FLAG tagged PB1-F2 proteins or eGFP and chicken MAVS-V5. Transects
879 were drawn in both the MAVS and PB1-F2/ eGFP channel and colocalisation via pixel
880 intensity were compared using a Pearson correlation coefficient. Pearson's correlation
881 coefficient (R^2) values from ten cells for each PB1-F2 construct and eGFP were averaged
882 and plotted. 1 way ANOVA was used to determine if significant difference in the
883 correlations existed. ****= P< 0.0005. (b) DF1 cells were co-transfected with PB1-F2-
884 FLAG and chicken MAVS–V5 expression constructs in varying combinations as shown.

The input expression levels of PB1-F2 and ckMAVS plus the resultant co-immunoprecipitation pulled down proteins on protein G beads by an anti-V5 antibody. This image is representative of the experiment which was performed twice. (c) UV inactivated cell supernatants from high MOI influenza virus infections of BMDMs were serially diluted (Log_2) and incubated on DF-1 cells for 12 h. Cells were washed and incubated with VSV-GFP virus for 12 h and fluorescence was read at 560 nm. The means +/- SD are shown. This data is representative of at least two independent repeats. Viruses were isogenic pairs of H5N1 5092 and H9N2 UDL01 with point mutation to knockout functional full length PB1-F2 protein (Ko – Blue) or wild type PB1-F2 coding capacity (Wt – Red). Mock samples were uninfected cell supernatants. (d) DF-1 cells were transfected with a chicken IFN-2 promoter firefly luciferase reporter, constitutively active Renilla expression plasmid and 2µg of PB1-F2 overexpression plasmid. 12 hrs post transfection cells were re-transfected with 0.25 µg of poly (I:C). At 24 hrs post transfection cells were lysed and luciferase activities quantified. The luciferase intensities were normalised to Renilla expression. The means of three independent experiments +/- SD and One-way ANOVA analysis was performed, ** indicates $p<0.005$, ns indicates not significant.

Fig. 5. Co-localisation of PB1-F2 with the mitochondria reduced interaction with IKKβ and antagonism of NFκB activity. (a) DF-1 cells were transfected with an NFκB dependent promoter firefly luciferase reporter, constitutively active Renilla expression plasmid and 2µg V5-PB1-F2 overexpression plasmid. 12 hrs post transfection cells were stimulated with poly (I:C). At 24 hrs post transfection cells were lysed and luciferase activities quantified. The luciferase intensities were normalised to Renilla expression. The means of three independent experiments +/- SD and One-way ANOVA analysis was

908 performed, ** indicates p<0.005, ns indicates not significant. (b) DF1 cells were co-
909 transfected with V5-PB1-F2 and chicken IKKβ-FLAG expression constructs in varying
910 combinations as shown. The input expression levels of V5-PB1-F2 and ckIKKβ-FLAG
911 plus the resultant co-immunoprecipitation pulled down proteins on protein G beads by an
912 anti-FLAG antibody. This image is representative of the experiment which was performed
913 twice. (c) DF-1 cells were transfected with combinations of ckIKK-β-Flag and V5-PB1-F2
914 expression plasmids. 12 hpt cells were fixed and immunostained with antibodies against
915 FLAG (ckIKK-β [Red]) and V5 (PB1-F2 [Green]) and stained with DAPI (Nucleus [Blue]).
916 (d) Pearson's correlation coefficients of ckIKK-β-Flag and V5-PB1-F2 co-localisation were
917 calculated. This was performed for at least fifteen separate images from two independent
918 experiments and displayed graphically. Significance were calculated using a student's t-
919 test, **** indicates p≤0.0001.

920 **Fig. 6. Stability of PB1-F2 protein in chicken cells.** (a) DF-1 cells were transfected with
921 expression plasmids for H9N2 UDL01 and H5N1 5092 PB1-F2 V5 tagged proteins. At 24
922 hours post transfection cycloheximide was applied to the cells and then cells lysed at
923 various time-points as indicated. Lysates were run on western blot and probed for V5
924 (PB1-F2) and actin as a loading control. (b) Cycloheximide chase assay was performed
925 on DF-1 cells transfected with various Wt, C-terminal swap and 4M PB1-F2 mutants as
926 indicated. Levels of V5-PB1-F2 at time of cycloheximide addition (0 hrs) and 1 hour were
927 probed using anti-V5 antibody and actin as a loading control. (c) Densitometry was
928 performed on the V5-PB1-F2 band of the cycloheximide chase assay for both 0 and 1
929 hour time points. Signal was normalised for actin and 0 hours for each V5-PB1-F2
930 construct set to 1. Relative V5- PB1-F2 levels at 1 hours post cycloheximide addition was

calculated and graphically represented. Average of three independent repeats displayed and standard deviation indicated by error bars. Significance were calculated using a student’s t-test, *** indicates p≤0.0005, ns is not-significant.

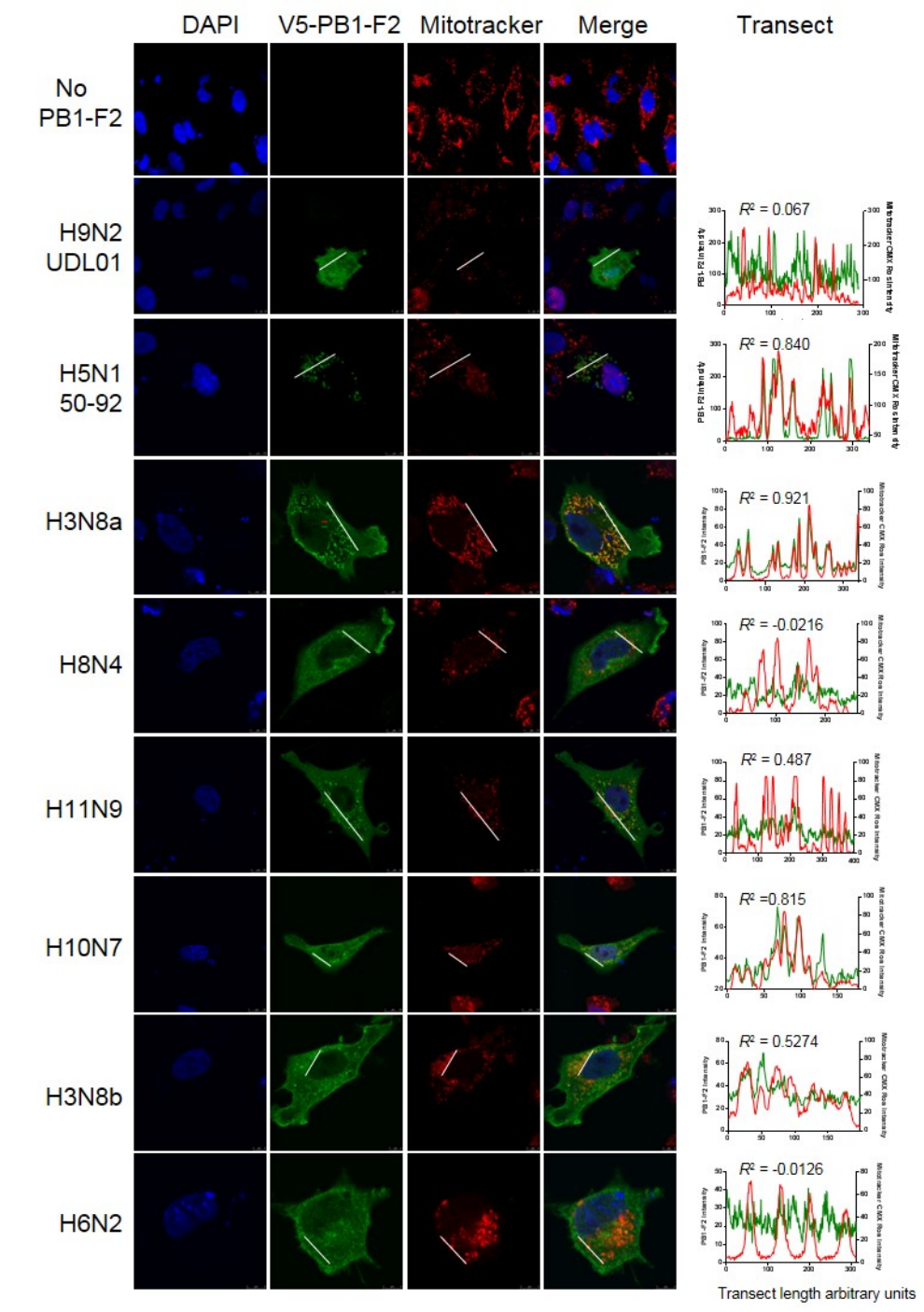
DAPI
V5-PB1-F2
Mitotracker
Merge
Transect
No PB1-F2
H9N2 UDL01
H5N1 50-92
H3N8a
H8N4
H11N9
H10N7
H3N8b
H6N2
R² = 0.067
R² = 0.840
R² = 0.921
R² = -0.0216
R² = 0.487
R² =0.815
R² = 0.5274
R² = -0.0126
Transect length arbitrary units

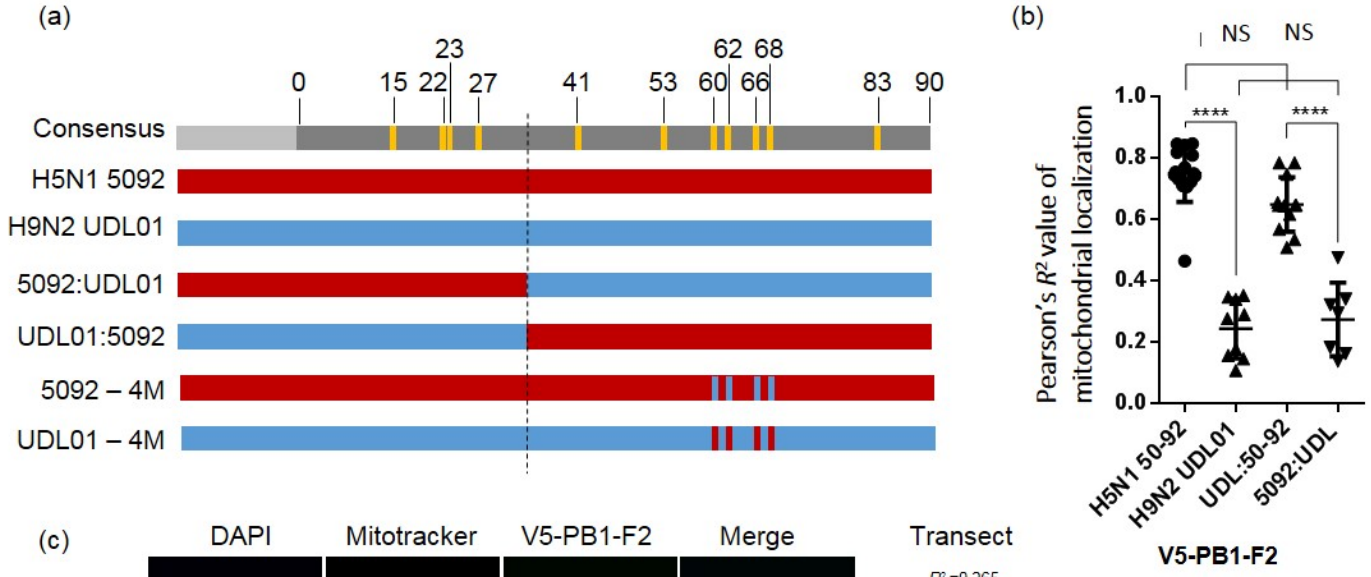

(d)

	45			50								60	62			66	68														90	Mito	Leucines
H3N8a A/mallard/Alberta/156/01	T	M	S	Q	V	D	M	H	K	R	T	V	S	L	K	Q	W	L	S	L	K	S	P	T	Q	E	S	L	K	T	R	V	L	K	R	W	K	L	S	N	K	Q	E	W	T	N	Y	6
H10N7 A/duck/Italy/1398/06	T	T	S	Q	A	D	M	H	K	R	I	A	C	W	K	Q	W	L	S	L	K	N	P	T	Q	G	S	L	K	T	L	V	L	R	R	W	K	S	F	S	K	Q	E	W	T	N	Y	5
H5N1 A/turkey/England/50-92/1991	I	T	S	Q	A	D	M	H	K	Q	I	V	C	W	K	Q	W	L	S	L	K	S	P	T	Q	G	S	L	K	T	H	V	L	K	R	W	K	L	F	S	K	Q	E	W	I	N	Y	5
H1N1 A/Puerto Rico/8/34	T	M	N	Q	V	V	M	P	K	Q	I	V	Y	W	R	R	W	L	S	L	R	N	P	I	L	V	F	L	K	T	R	V	L	K	R	W	R	L	F	S	K	H	E	W	T	S	Y	6
H9N2 A/chicken/Pakistan/UDL-01/2008	I	T	S	Q	A	D	M	H	R	Q	I	V	C	W	K	R	W	H	S	L	K	N	P	I	Q	G	S	L	K	T	H	V	L	K	R	W	K	L	S	S	K	Q	E	W	I	N	N	5
H3N8b A/duck/Italy/3139/06	I	T	S	Q	A	D	M	H	K	Q	I	A	C	W	K	Q	W	L	S	L	K	N	P	T	Q	G	S	L	K	T	H	V	L	R	R	W	K	L	F	S	K	Q	E	W	I	N	N	5
H8N4 A/mallard/Alberta/194/92	I	M	S	Q	V	D	M	H	K	Q	T	V	S	W	K	Q	W	L	S	L	K	S	P	T	Q	E	S	S	K	T	R	V	S	K	R	W	K	L	F	N	K	Q	E	W	T	S	N	3
H6N2 A/duck/Italy/2253/06	I	M	N	Q	V	D	M	H	K	Q	T	V	S	W	K	Q	W	L	S	L	K	N	P	T	Q	E	S	L	K	T	R	V	L	K	R	W	K	L	S	N	K	Q	G	W	T	S	N	5
H11N9 A/duck/Italy/6103/07	T	T	S	Q	V	D	M	H	K	R	I	A	C	W	K	Q	W	L	S	L	K	N	P	T	Q	G	S	L	K	T	L	V	L	K	R	W	K	L	F	S	K	Q	E	W	T	N	N	6
H5N1 A/Hong Kong/156/1997	I	T	S	R	A	G	M	H	K	Q	I	V	Y	W	K	Q	W	L	S	L	K	N	P	T	Q	D	S	L	K	T	H	V	L	K	R	W	K	L	S	S	K	R	E	W	I	S	N	5

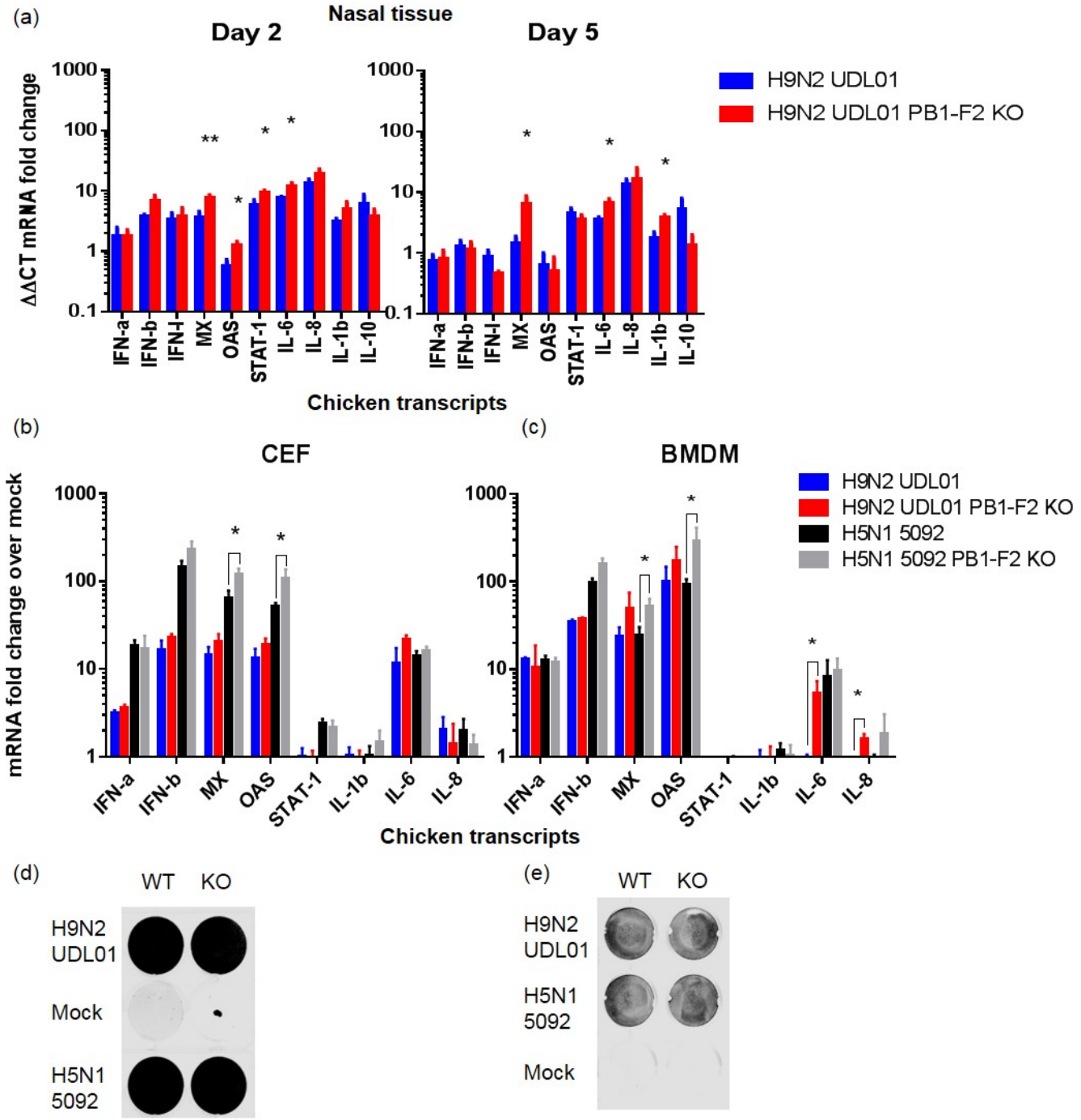
(a)
Nasal tissue
Day 2
Day 5
ΔΔCT mRNA fold change
1000
100
10
1
0.1
**
*
*
*
*
*
*
IFN-a
IFN-b
IFN-l
MX
OAS
STAT-1
IL-6
IL-8
IL-1b
IL-10
Chicken transcripts
H9N2 UDL01
H9N2 UDL01 PB1-F2 KO
(b)
CEF
(c)
BMDM
mRNA fold change over mock
H5N1 5092
H5N1 5092 PB1-F2 KO
(d)
WT
KO
H9N2 UDL01
Mock
H5N1 5092
(e)

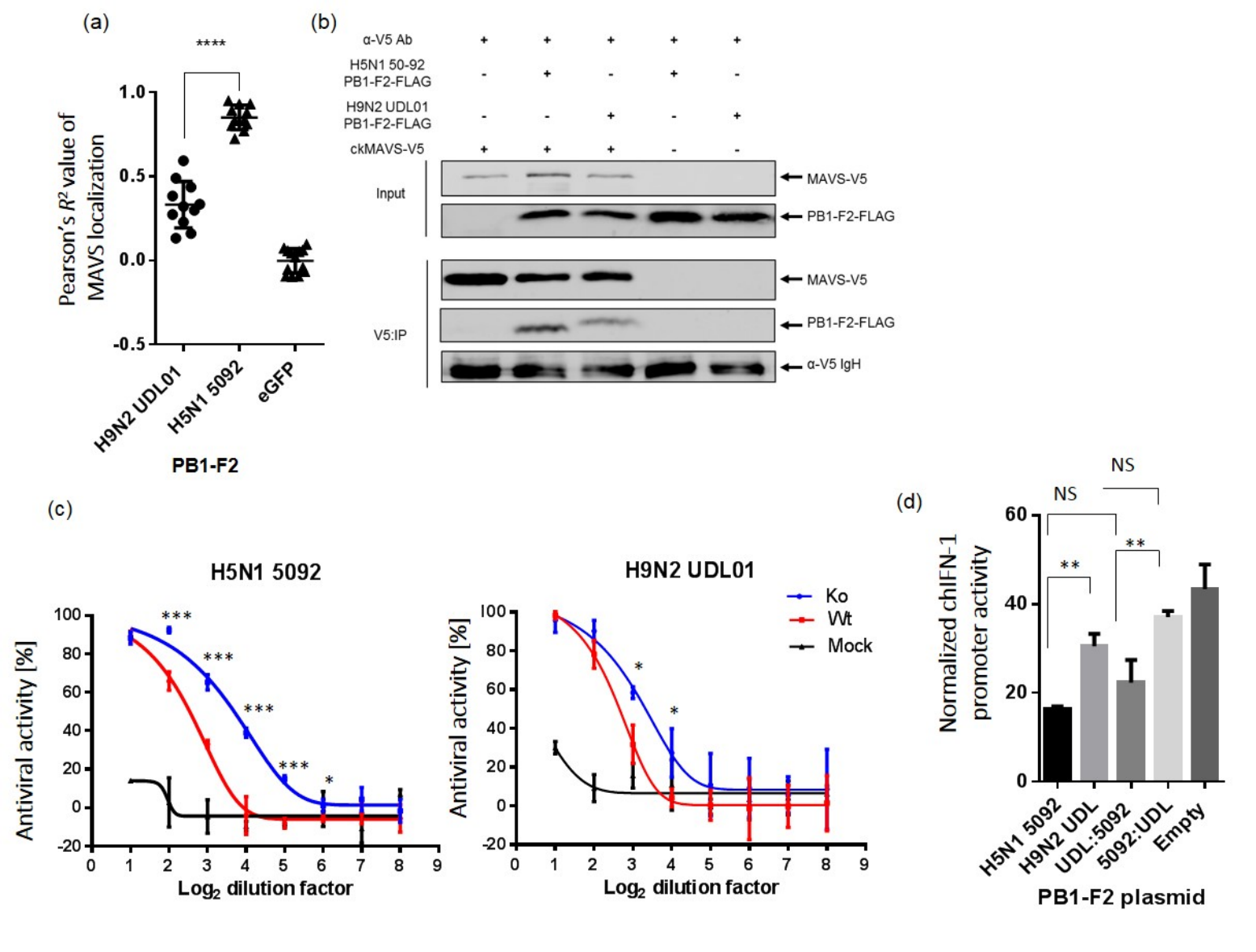
(a)
****
Pearson's R^2 value of MAVS localization
1.0
0.5
0.0
-0.5
H9N2 UDL01
H5N1 5092
eGFP
PB1-F2
(b)
α-V5 Ab
H5N1 50-92 PB1-F2-FLAG
H9N2 UDL01 PB1-F2-FLAG
ckMAVS-V5
Input
V5:IP
MAVS-V5
PB1-F2-FLAG
MAVS-V5
PB1-F2-FLAG
α-V5 IgH
(c)
H5N1 5092
H9N2 UDL01
Ko
Wt
Mock
Antiviral activity [%]
Log2 dilution factor
(d)
NS
NS
**
**
Normalized chIFN-1 promoter activity
H5N1 5092
H9N2 UDL
UDL:5092
5092:UDL
Empty
PB1-F2 plasmid

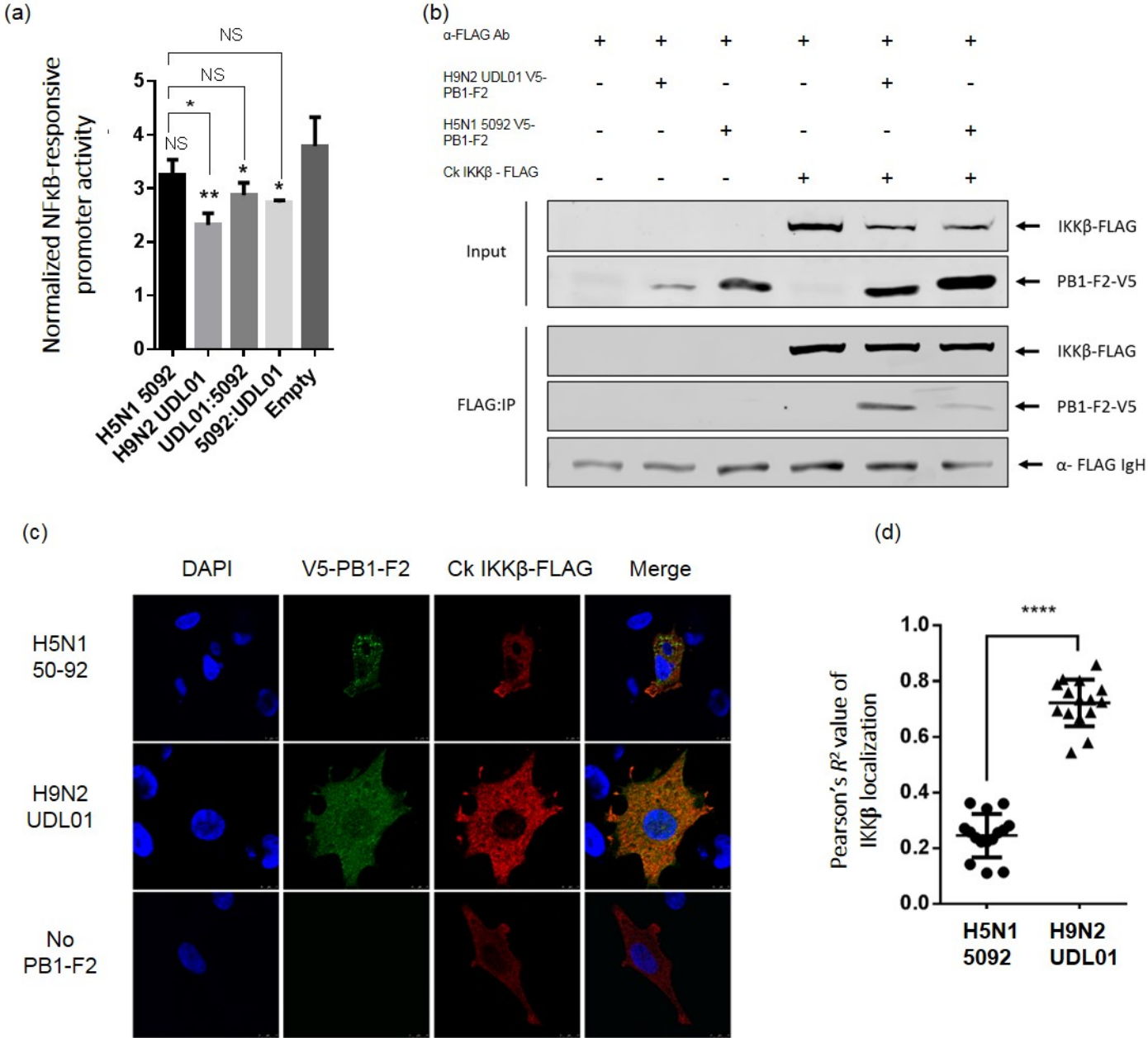
(a)
Normalized NFκB-responsive promoter activity
NS
NS
NS
*
**
*
*
5
4
3
2
1
0
H5N1 5092
H9N2 UDL01
UDL01:5092
5092:UDL01
Empty
(b)
α-FLAG Ab
H9N2 UDL01 V5-PB1-F2
H5N1 5092 V5-PB1-F2
Ck IKKβ - FLAG
Input
FLAG:IP
IKKβ-FLAG
PB1-F2-V5
IKKβ-FLAG
PB1-F2-V5
α- FLAG IgH
(c)
DAPI
V5-PB1-F2
Ck IKKβ-FLAG
Merge
H5N1 50-92
H9N2 UDL01
No PB1-F2
(d)
****
Pearson's R² value of IKKβ localization
1.0
0.8
0.6
0.4
0.2
0.0
H5N1 5092
H9N2 UDL01

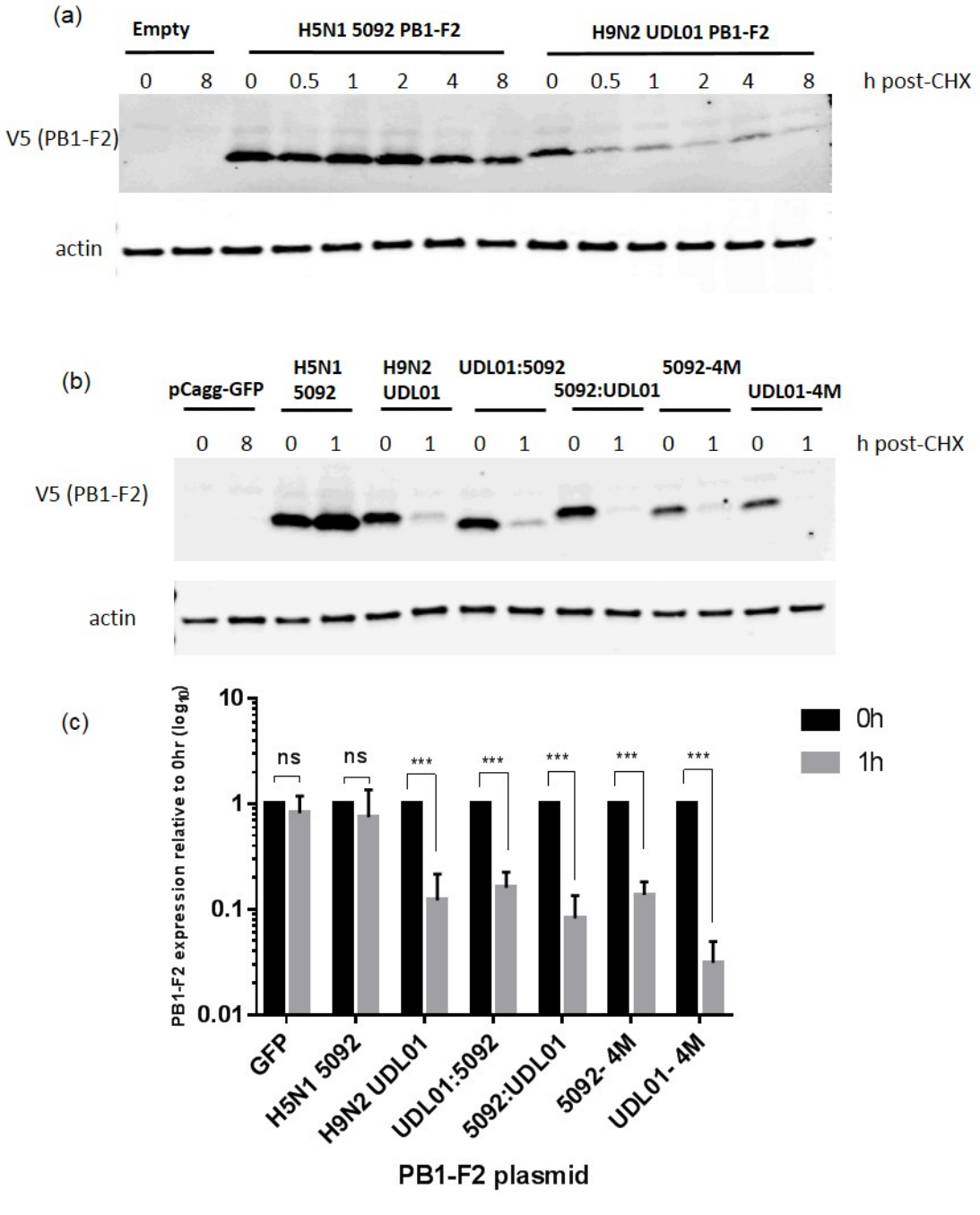
(a)
Empty
H5N1 5092 PB1-F2
H9N2 UDL01 PB1-F2
0 8 0 0.5 1 2 4 8 0 0.5 1 2 4 8
h post-CHX
V5 (PB1-F2)
actin
(b)
pCagg-GFP
H5N1 5092
H9N2 UDL01
UDL01:5092
5092:UDL01
5092-4M
UDL01-4M
0 8 0 1 0 1 0 1 0 1 0 1 0 1
h post-CHX
V5 (PB1-F2)
actin
(c)
PB1-F2 expression relative to 0hr (log10)
10
1
0.1
0.01
ns
ns
***
***
***
***
***
0h
1h
GFP
H5N1 5092
H9N2 UDL01
UDL01:5092
5092:UDL01
5092- 4M
UDL01- 4M
PB1-F2 plasmid

Supplementary Figures.

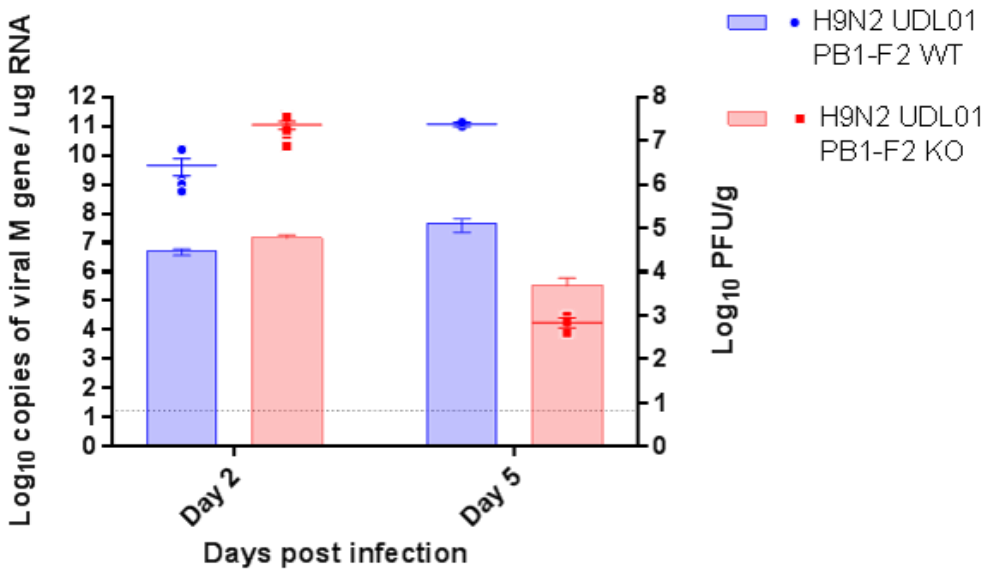

Supplementary Fig. 1. Virus load in chicken nasal tissue. Left axis – Dots and squares indicates copies of viral M gene mRNA determined via influenza specific RT-qPCR on total nasal tissue RNA. Tissues were harvested and processed at 2 or 5 dpi following infection of chickens with 1 x105 pfu of either H9N2 UDL01 PB1-F2 WT (Blue) or H9N2 UDL01 PB1-F2 KO (Red) virus. Right axis – Bars Infectious virus in the nasal tissue was determined by virus titration on MDCK cells following homogenisation. Infectious virus titre was normalised by weight of tissue sample. Grey dotted lines indicate plaque assay limit of detection. Means ±SD were calculated from a minimum of three individual animals.

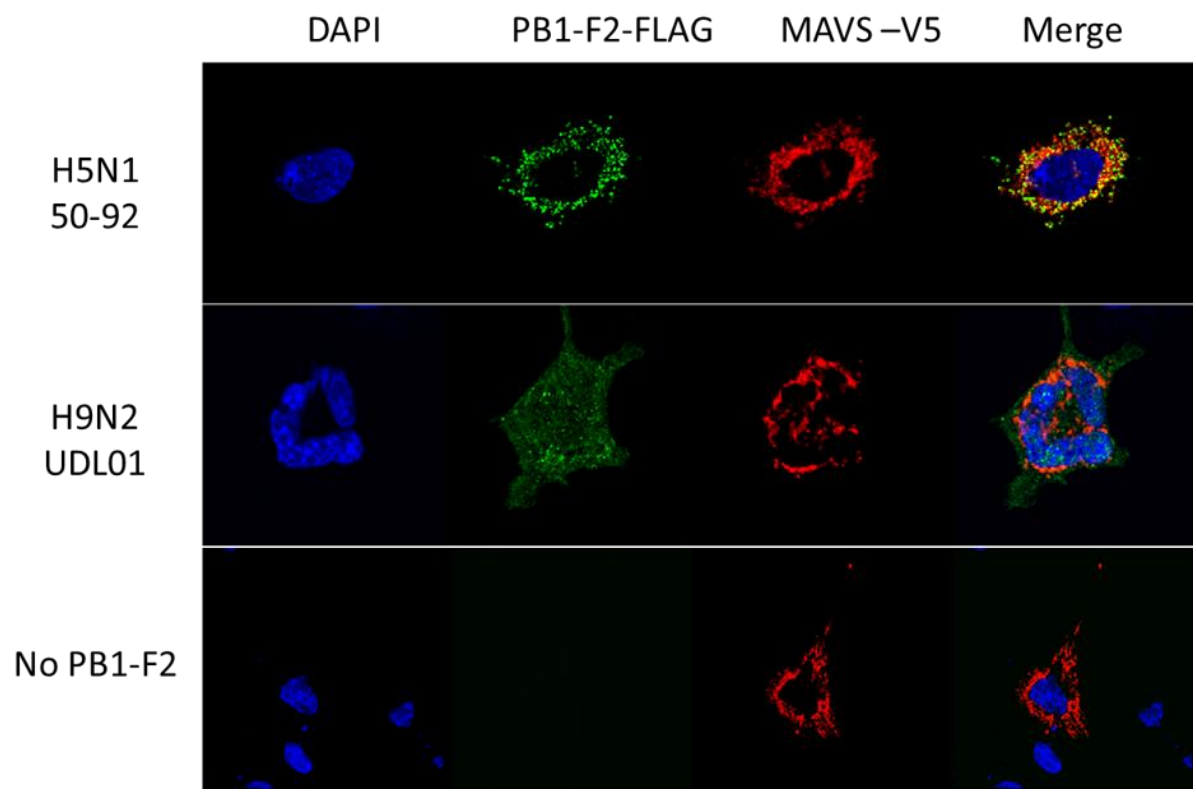

Supplementary Fig. 2. Co-localisation of PB1-F2 and chicken MAVS. DF-1 cells were transfected with combinations of ckMAVS-V5 and FLAG-PB1-F2 expression plasmids. 12 hpt cells were fixed and immunostained with antibodies against V5 (ckMAVS [Red]) and FLAG (PB1-F2 [Green]) and stained with DAPI (Nucleus [Blue]).

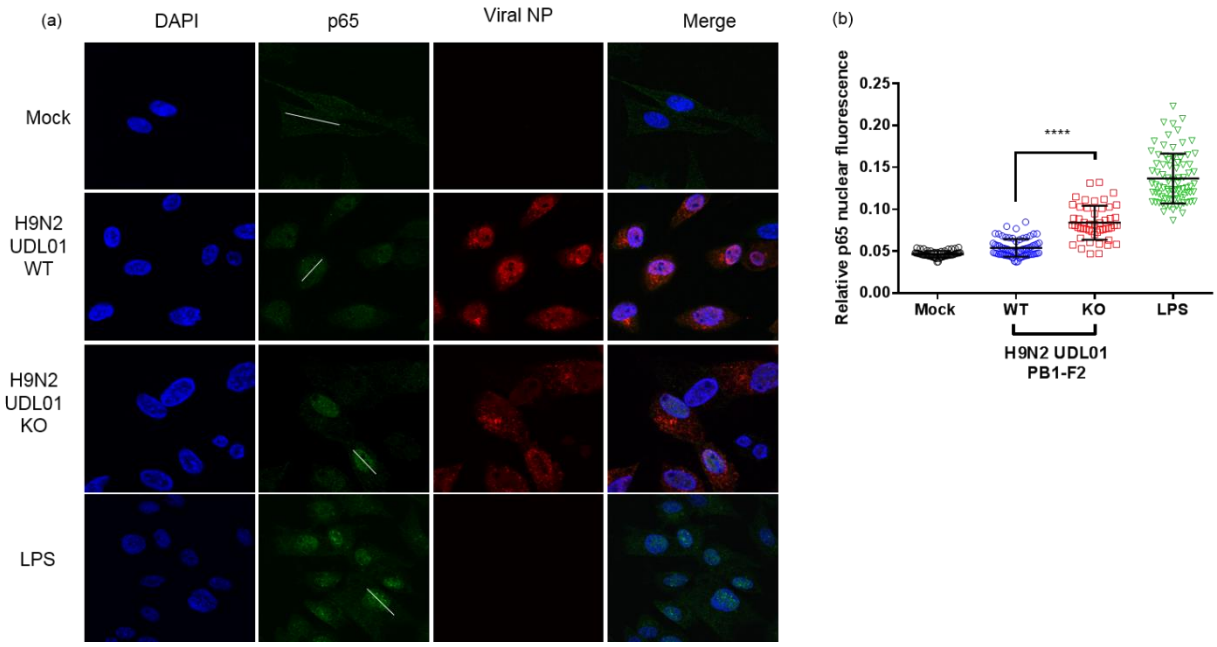

Supplementary Fig. 3. The presence of PB1-F2 in H9N2 UDL01 influenza virus inhibits the nuclear translocation of NFκB p65 in chicken cells during influenza virus infection. (a) Chicken kidney cells were infected with H9N2 UDL01 WT or H9N2 UDL01 PB1-F2 KO virus and immunostained with anti-p65 (green) and influenza nucleoprotein (NP) (red) antibodies at 3 hpi. (b) The nuclear intensity of p65 was calculated relative to the surrounding cytoplasmic intensity for infected cells. Means ±SD were calculated from least 30 random cells for each condition was measured and displayed graphically. Significance were calculated using a student's t-test, **** indicates p≤0.0001.

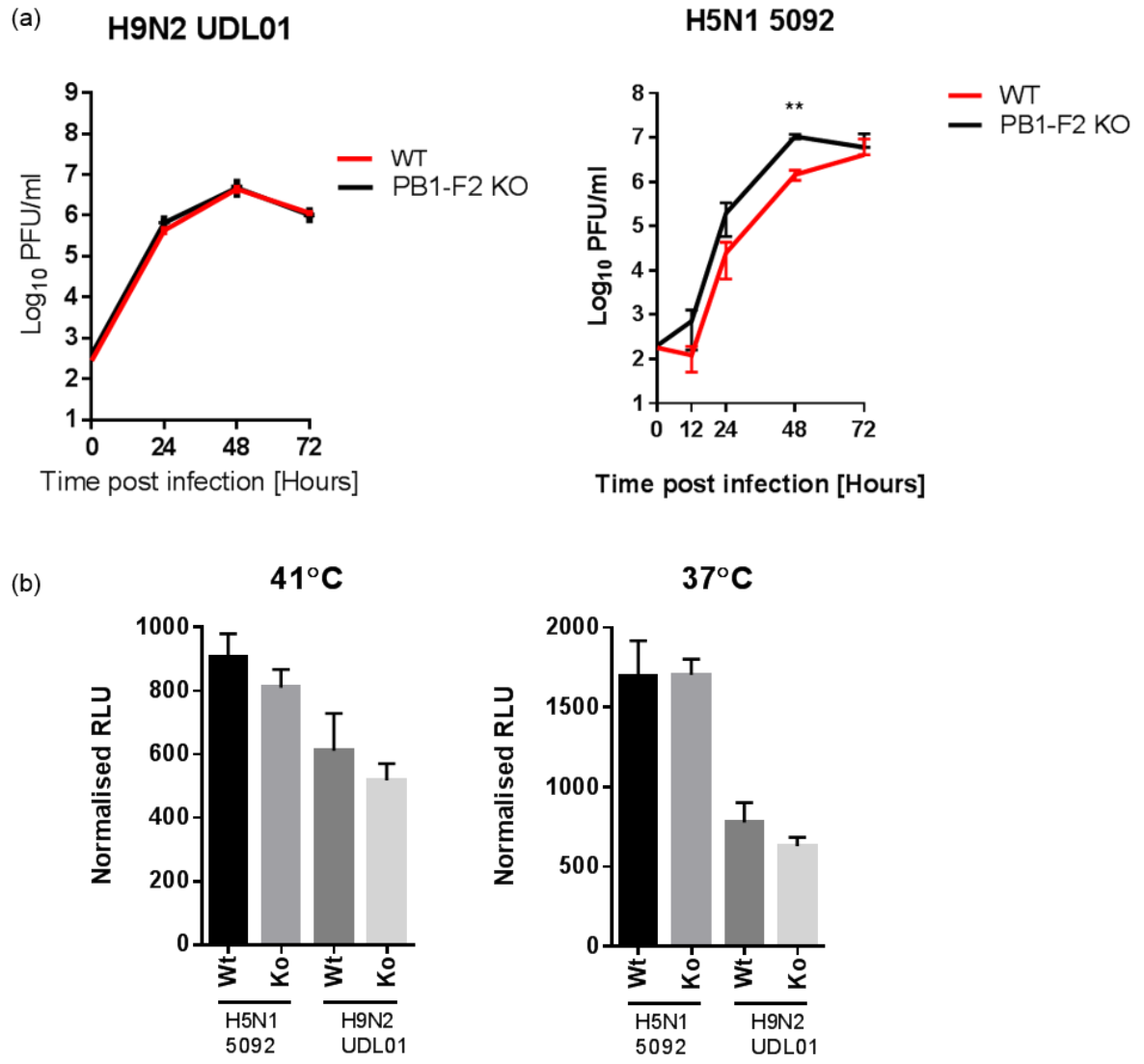

Supplementary Fig. 4. Absence of PB1-F2 does not affect viral polymerase activity in avian cells. (a) Primary chicken kidney cells were inoculated with isogenic viruses differing by the presence of PB1-F2 of either the H9N2 UDL01 strain or H5N1 5092 strain at an MOI 0.0001 at 37°C. Cell supernatant was collected at the indicated time-points and titrated on MDCK cells for infectious virus, plaque forming units (Log_{10}PFU/ml). WT (Red) contains a full length PB1-F2, PB1-F2 KO (black) is the functional PB1-F2 knock out virus. (b) In triplicate, DF-1 cells were transfected with viral polymerase expression plasmids, the PB1 plasmids encoding the ability to express PB1-F2 (WT) or not (Ko) in addition to PB1 and PB1-N40, from H9N2 UDL01 or H5N1 5092. A firefly luciferase reporter for the viral RNA-dependant-RNA polymerase in chicken cells was used to determine polymerase transcriptional activity at either 41°C or 37°C.